Journal of Analytical and Applied Pyrolysis 192 (2025) 107329

Contents lists available at ScienceDirect

Journal of Analytical and Applied Pyrolysis

journal homepage: www.elsevier.com/locate/jaap

Improving bio-oil fractions through fractional condensation of pyrolysis vapors from *Eucalyptus globulus* biomass residues in a prototype auger reactor

A.C.M. Vilas-Boas [a,*], L.A.C. Tarelho [a], C.C. Marques [a], J.M.O. Moura [a], M.C. Santos [a,b], F. Paradela [c], M.I. Nunes [a], A.J.D. Silvestre [d]

[a] Department of Environment and Planning & Centre for Environmental and Marine Studies (CESAM), University of Aveiro, Aveiro, Portugal
[b] Laboratory of Ceramic Materials - LACER, Materials Engineering Department, Federal University of Rio Grande do Sul, Porto Alegre, Brazil
[c] Bioenergy and Biorefineries Unit, National Laboratory of Energy and Geology - LNEG, Lisboa, Portugal
[d] Department of Chemistry & CICECO-Aveiro Institute of Materials, University of Aveiro, Aveiro, Portugal

ARTICLE INFO

Keywords:
Bio-oil fractions
Eucalyptus globulus residual biomass
Eucalyptus globulus branches
Eucalyptus globulus leaves
Fractional condensation
Water separation efficiency

ABSTRACT

Bio-oil produced from the pyrolysis of lignocellulosic biomass has potential as a biofuel or chemical precursor. However, its valorization is hindered by its complex composition, high water concentration, and the presence of oxygenated compounds. Operational strategies are therefore required to improve its quality. This study evaluated the technical feasibility of fractional condensation as an alternative to conventional single-stage condensation of vapors produced from pyrolysis of residual *Eucalyptus globulus* biomass to collect bio-oil fractions with improved properties. The process was carried out using a prototype-scale auger reactor with continuous operation. The fractional condensation system comprised four sequential condensation stages operating at progressively lower temperatures: 140, 100, 80, and 0 ºC. The collected bio-oil fractions were analyzed in terms of product yields, water separation efficiency, elemental composition, heating value, and the presence of volatile and semi-volatile compounds. The results demonstrated that fractional condensation achieved total bio-oil yields comparable to those obtained with the single-stage condensation system, while enabling the recovery of bio-oil fractions with lower water concentration, higher carbon concentration and increased heating value. Notably, the first condensation stage collected heavy fractions with water concentration between 3 % and 6 %wt., oxygen concentration between 17 % and 21 %wt., and carbon concentration between 69 % and 72 %wt., resulting in O/C molar ratios between 0.17 and 0.22, values close to those of biodiesel. These fractions exhibited lower heating values of up to 31 MJ/kg, surpassing those of conventional liquid biofuels such as biomethanol and bioethanol. These findings highlight the potential of fractional condensation of pyrolysis vapors from residual biomass from *Eucalyptus globulus* as an effective strategy to produce bio-oil with properties more suitable for direct energy use or as an intermediate feedstock for biofuels synthesis. Further research is recommended to optimize the condensation stages and assess the long-term stability of recovered fractions.

1. Introduction

Wildfires are a major concern in Europe, particularly in the Iberian Peninsula. Between 2014 and 2023, an average of 404,000 ha of forest burned annually across Europe, with 198,000 ha located in the Iberian Peninsula, of which 109,000 ha per year in Portugal alone [1]. In 2023, 36,498 ha burned in Portugal [2]. Although below average, these fires caused an estimated public economic loss of nearly €400 million [3]. Beyond the economic impact, wildfires result in significant human losses and substantial greenhouse gas emissions. For instance, the Pedrógão Grande fire in Portugal, in 2017 caused 66 fatalities and over 253 injuries [4]. That year, wildfire related emissions were estimated at 21.5 $MtCO_2e$, surpassing emissions from the transport sector (≈17 $MtCO_2e$) [5].

Therefore, sustainable forest management emerges as a key strategy to reduce wildfire risk by minimizing the accumulation of combustible biomass on the forest soil. In mainland Portugal, approximately 26 % of the forest area is occupied by eucalyptus plantations [6], whose wood is the main raw material for the pulp and paper industry, which includes

* Corresponding author.
E-mail address: catarina.vilas.boas@ua.pt (A.C.M. Vilas-Boas).

https://doi.org/10.1016/j.jaap.2025.107329
Received 20 May 2025; Received in revised form 8 July 2025; Accepted 12 August 2025
Available online 16 August 2025

Nomenclature

db	Dry basis
DME	Dimethyl ether
EB	Eucalyptus globulus branches
EL	Eucalyptus globulus leaves
HF	Heavy fraction
HHV	Higher heating value
LF	Light fraction
LHV	Lower heating value
LPG	Liquefied petroleum gas
FCS	Fractional condensation system
MW_R	Molecular weight relative (g/mol)
NPT	Standard pressure (1.013×10^5 Pa) and temperature (273 K) conditions
RBE	*Eucalyptus globulus* residual biomass
SAF	Sustainable aviation fuels
SCS	Single-stage condensation system
S1	Stage 1
S2	Stage 2
S3	Stage 3
S4	Stage 4
wb	Wet basis
$\dot{m}_{BC}$	Mass flow rate of biochar, kg/h
$\dot{m}_{BM}$	Mass flow rate of fed biomass, kg/h
$\dot{m}_{BO}$	Total mass flow rate of bio-oil collected in the experiment, kg/h
$\dot{m}_{BO_1}$	Mass flow rate of vapor precursors of bio-oil in stream 1, kg/h
$\dot{m}_{BO_2}$	Mass flow rate of bio-oil collected in the condensation systems (stream 2), kg/h
$\dot{m}_{PG_1}$	Mass flow rate of vapor precursors of permanent gas in stream 1, kg/h
$\dot{m}_{PG_2}$	Mass flow rate of permanent gas downstream of the condensation systems (stream 2), kg/h
$\dot{m}_{V_1}$	Mass flow rate of pyrolysis vapors in stream 1, kg/h
$\dot{m}_{V_2}$	Mass flow rate of pyrolysis vapors in stream 2, kg/h
M_{PG2}	Molar mass of the permanent gas at the condensation system exit, kg/kmol
V_{G_2}	Volume flow rate of gas (permanent gas and purge N_2) downstream of the condensation systems, Nm^3/h
$\dot{V}_{PG_2}$	Volume flow rate of the permanent gas in stream 2, Nm^3/h
y_{GG_2}	Volumetric fraction of the permanent gas in the total measured gas (N_2 + permanent gas), Nm^3_{PG2}/Nm^3_{G2}
η_{BC}	Biochar yield, %wt.
$\eta_{BO_1-V_1}$	Bio-oil yield in stream 1, %wt.
$\eta_{BO_2-V_2}$	Bio-oil yield in stream 2, %wt.
η_{BO_T}	Total yield of bio-oil of experiment (stream 1 and 2), %wt.
$\eta_{PG_1-V_1}$	Permanent gas yield in stream 1, %wt.
$\eta_{PG_2-V_2}$	Permanent gas yield in stream 2, %wt.
η_{PG}	Total yield of permanent gas in the experiment (stream 1 and 2), %wt.

seven production units in the country [7]. Therefore, it is essential to develop technological solutions for the valorization of eucalyptus forestry residues, such as branches, bark, leaves, and sawdust, promoting their economic use, increasing forest value and preventing their abandonment in the field.

Traditionally, residual biomass from forest management has been used in combustion boilers to generate steam and electricity, supporting industrial operations while, in some cases, supplying surplus energy to the power grid [8,9]. However, this residual biomass holds significant potential for conversion into high value-added products, such as biofuels and biochemicals, which can replace fossil fuels and increase the economic value of forestry residues [9–11]. Adopting such innovative approaches enables the pulp and paper industry to diversify its portfolio and move toward more comprehensive biorefinery models, producing a variety of outputs (e.g., pulp, paper, fuels and chemicals) from a single feedstock [9]. This transformation represents a strategic step in the context of the energy transition and the sustainable economy, in line with the United Nations Sustainable Development Goals [12] and European strategic initiatives, such as the European Green Deal and the REPowerEU program, which aims to achieve Europe's energy independence from fossil fuels by 2030 [13,14].

In this context, pyrolysis of residual biomass emerges as a promising sustainable thermochemical technology capable of producing a variety of bioproducts [15–19], including biodiesel, sustainable aviation fuels (SAF), marine biofuels, biogasoline, and biobased chemicals for diverse applications in the chemical industry [17,18,20,21]. Pyrolysis involves thermal decomposition of biomass at 400–600 °C in an oxygen-free atmosphere, generating three primary products: biochar, bio-oil, and permanent gases [22]. Biochar is particularly valued for its carbon sequestration potential and its applications in soil restoration, while bio-oil offers potential as a renewable fuel and as a precursor for chemicals, and may be co-processed in conventional petrochemical refineries.

However, the direct use of bio-oil remains limited by its complex composition. It typically contains a high oxygen concentration and reactive compounds such as aldehydes and acids, which can lead to polymerization of bio-oil components, increased viscosity over time and overall instability [23]. In addition, bio-oil often contains a high water concentration, frequently exceeding 50 %wt. [24], which compromises its applicability in certain uses.

To overcome these limitations, several strategies have been studied to stabilize and improve bio-oil properties. These include catalytic pyrolysis, fractionation techniques such as fractional condensation of pyrolysis vapors and bio-oil distillation, and hydrodeoxygenation [25,26]. In catalytic pyrolysis, commercial catalysts such as zeolites have been applied both *in situ* (during pyrolysis) and *ex situ* (after the formation of pyrolysis vapors or bio-oil) to promote cracking of high-molecular-weight compounds and partial deoxygenation of volatile products. Hydrodeoxygenation involves treating bio-oil under high pressures in the presence of catalysts and large amounts of hydrogen to reduce its oxygen concentration, thereby enhancing its stability, energy density, and compatibility with conventional refining systems. Fractional condensation uses a series of condensers operating at different temperatures to sequentially separate the vapors produced during pyrolysis into distinct fractions with improved physicochemical properties [27–30]. Among these strategies, fractional condensation stands out as particularly attractive for decentralized or modular pyrolysis systems due to its operational simplicity, low energy requirements, and ability to selectively recover more stable, energy-rich fractions without the need for catalysts or pressurized systems [29]. Additionally, this technique can be integrated with other upgrading processes, functioning as a pre-separation step for pyrolysis vapors, which contributes to cost reduction and enables more targeted and efficient downstream treatments.

Fractional condensation offers clear advantages over conventional single-stage condensation systems by enabling the separation of bio-oil fractions with potentially lower water and oxygen concentration, depending on the volatility and chemical composition of the vapors [29,30]. Unlike conventional single-stage condensation systems, fractional condensation uses a series of condensers operating at progressively

lower temperatures. As pyrolysis vapors pass through this sequence, compounds with different volatilities are selectively recovered, resulting in bio-oil fractions with distinct physicochemical profiles [31,32]. Despite its simplicity and potential, the effective separation of water and oxygenated functional groups remains a challenge due to the complex composition of pyrolysis vapors. Optimization of the condensation stages temperatures, number of condensers, and vapor residence time, along with robust analytical methodologies for characterizing the resulting bio-oil fractions is essential for advancing this technology [33,34].

Previous studies have explored fractional condensation systems with two to four condensers operating across wide temperature ranges (Table 1) [28,35–39]. Generally, high-temperature stages (>100 °C) recover heavy fractions with higher molecular weight compounds, lower water concentration, and, consequently, higher heating value, while low-temperature stages collect fractions rich in light compounds, with higher acidity, water, and oxygen concentrations [36,40]. For example, Chai *et al.* [35] used a bubbling fluidized bed pyrolysis reactor coupled with four-stage vapor condensation (200 °C, 150 °C, −5 °C, −20 °C) and found that early stages produced bio-oil with higher pH (6.1–6.6) and lower water concentration (<3 %wt.), while latter stages at lower temperatures yielded water-rich bio-oil (>35 %wt.) with lower pH values (4.2–4.7). Li *et al.* [38] reported similar findings with two-stage system operating at 85 °C and −10 °C. Mati *et al.* [28], using a three-stage system, noted higher Higher Heating Value (HHV, 21–25 MJ/kg) and lower oxygen concentration in bio-oil fractions at higher temperature, while the fractions obtained at the lowest temperature stage had significantly lower HHV (6–7 MJ/kg). Conversely, other studies using auger reactors and multi-stage condensation [39,41], found similar pH across fractions and shifts in compounds families, such as reduced phenolics and increased anhydrous sugars at lower temperatures. While these studies provide valuable insights, the lack of comprehensive investigations combining detailed physicochemical characterization with fractionation analysis limits a full understanding of the composition and potential applications of individual bio-oil fractions.

This gap is particularly evident in studies involving prototype-scale auger reactors, where design and operating conditions, such as, biomass type, pyrolysis temperature, and nitrogen flow rate, strongly influence vapor composition and condensation behavior. Moreover, eucalyptus biomass residues, particularly from *Eucalyptus globulus*, remain underexplored, despite their relevance in the Iberian Peninsula's forest landscape and high valorization potential. Their relatively high lignin and extractives content, especially in leaves, can promote the formation of terpenes and phenolics compounds during pyrolysis [22,36,37,42], significantly affecting the distribution and properties of bio-oil fractions, requiring tailored condensation strategies.

In this context, the present study aims to advance knowledge on fractional condensation applied to pyrolysis vapors from residual *E. globulus* biomass, including material from agroforestry management practices, using a prototype-scale auger reactor equipped with a four-stage condensation system. The novelty of this work lies in the simultaneous assessment of the technical feasibility of this approach under realistic operational conditions and the influence of the biomass composition on the physicochemical properties of the resulting bio-oil fractions.

The study tests the hypothesis that four-stage fractional condensation, operating at different temperatures, can generate higher-quality bio-oil fractions when compared to conventional single-stage condensation near 0 ºC, by recovering bio-oil fractions with lower water and oxygen concentration, and, consequently, higher heating value. This would bring the fractions closer to the specifications required for direct energy use or further upgrading into drop-in biofuels. Therefore, the use of this technique may contribute to reducing costs associated with additional upgrading steps. In this context, physicochemical parameters were analyzed, including water concentration, elemental composition, heating value, and distribution of organic compounds across light and heavy bio-oil fractions.

Thus, the results obtained support the development of pyrolysis technologies at industrial scales for the production of higher-quality bio-oil from residual eucalyptus biomass. They also contribute to fostering the valorization of this biomass into higher-value products, thereby promoting the circular bioeconomy and helping to mitigate wildfire risks.

2. Materials and methods

2.1. Feedstocks characterization

Residual biomass from *E. globulus* (RBE), derived from forestry operations of maintenance and logging, was used as feedstock. The studied biomass fraction comprised *E. globulus* branches (EB) from treetops with leaves, and *E. globulus* leaves (EL) obtained after essential oil extraction by hydrodistillation. The biomass was air-dried, crushed and sieved to particle sizes greater than 1 mm.

The macroscopic appearance of the dried and chipped RBE samples is shown in Fig. 1. Macroscopically, the EL exhibited a more homogeneous size distribution.

The samples were characterized through proximate analysis, which included measurement of moisture content (CEN/TS standards 14774–3:2004), volatile matter (CEN/TS standards 15148:2005), and ash content (CEN/TS standards 14775:2004). Fixed carbon was calculated by difference. In addition, elemental analysis was carried out to determine the concentrations of carbon, hydrogen, nitrogen and sulfur using an Elemental Analyzer (Model EA1108 Fisons Instruments). The oxygen concentration was estimated by difference, on a dry basis, and the empirical chemical formula of feedstock was determined based on its elemental composition. The Lower Heating Value (LHV) was determined using the correlation developed by Channniwala and Parikh [43].

The physicochemical properties of the biomass samples used in this study are presented in Table 2.

2.2. Experimental setup

2.2.1. Prototype-scale auger reactor

The experimental setup used in the experiments consisted of a prototype-scale auger reactor (Fig. 2) with processing capacity of 1 kg of residual forest biomass per hour. Its main characteristics have been described in previous work [44]. This experimental setup consisted of the main following components:

a) Biomass feeding: biomass is introduced into a V-type silo and transported to the pyrolysis section via a screw feeder driven by an electric motor. The rotation speed of the screw feeder is adjustable, allowing the precise control over the residence time of the biomass within the pyrolysis reactor.
b) Pyrolysis reactor: the reactor is an electrically heated unit with a total length of 0.5 m. The furnace temperature is pre-defined and controlled through a data acquisition and control system. Temperature monitoring is performed using a K-type thermocouple, which is in contact with the surface of the external wall of the pyrolysis reactor, located at the midpoint of the electric furnace.
c) Biochar discharge: the biochar produced during pyrolysis is discharged in a dedicated cylindrical silo located downstream of the pyrolysis section.
d) Vapors condensation and exhaust: the vapors exhaust system from the auger reactor is divided into two parallel circuits:
    i. Condensation System (CS): depending on the type of experiment – whether employing a fractional condensation system (FSC) or single-stage condensation system (SCS) – the setup includes a fractional condensation system module with three stages, three stainless steel condensers in series, Stage 1 (S1), Stage 2 (S2), and

Table 1
Summary of literature results of pyrolysis fractional condensation coupled systems with a processing capacity between 0.47 and 4 kg/h of feedstock.

		Chai *et al.* [35]	Mati *et al.* [28]	Liaw *et al.* [37]	Álvarez-Chávez *et al.* [36]	Li *et al.* [38]	Le Roux *et al.* [39]	Le Roux *et al.* [39]	Álvarez-Chávez *et al.* [41]	Siriwardhana [32]	Papari *et al.* [42]
Pyrolysis conditions	Biomass type	Five different types of sawdust	Pine wood	Douglas fir wood	Black spruce	Rice husk	Jerusalem artichoke stalk	White birch bark	Black spruce	Dry birch bark	Fresh softwood sawdust
	Biomass pre-treatment	Sieved to a size of 250 μm - 2 mm, and dried at 110 °C	Sieved to a size of 1–2 mm	Sieved to a size of 2 mm or less	Sieved to a size of 1.0–2.4 mm and dried at 105°C	Sieved to a size of 0.25 mm to 0.4 mm and dried in air	Sieved to a size of 1.1–3.5 mm and dried at 105 °C	Sieved to a size of 1.1–3.5 mm and dried at 105 °C	Sieved to a size of 1.0–2.4 mm and dried at 105 °C	Dry biomass about 1 mm	Sieved at 2 mm and dried at 75 °C
	Biomass composition	%wt. db M: 0.8–1.2 VM: 82.4–83.9 FC: 14.0–15.3 Ash: 0.5–2.1 %wt. db C: 49.35–52.69 H: 5.37–6.17 O: 40.2–42.7 N: 0.6–1.37 S: 0.02–0.06	M: 10 (wb) Ash: 2.6 C: 45.4 H: 6.18 O: 45.79 N: 0.04 S: 0.06	Ash: 0.3 C: 49.69 H: 7.35 O: 42.59 N: 0.06	Ash: 1.88 nd	M: 8.6 (wb) VM: 68.6 FC: 14.1 Ash:17.4 C: 34.67 H: 4.46 O: 45.65 N: 0.40	nd C:49.9 H: 6.3 N: 0.1 S: < 0.2	nd C: 63.3 H: 7.6 N: 0.4 S: 0.3	M: 3 (wb) Ash: 4.2 nd	nd nd	M: < 2 (wb) VM: 84.9 FC: 14.3 Ash:0.8 C: 47.92 H: 6.15 O: 45.12 N: 0.02
	Reactor type	Bubbling fluidized bed	Bubbling fluidized bed	Auger (horizontal auger reactor)	Auger (vertical auger reactor)	Bubbling fluidized bed	Auger (vertical auger)	Auger (vertical auger reactor)	Auger (vertical auger reactor)	Bubbling fluidized bed	Auger (horizontal auger reactor)
	Pyrolysis temperature (°C)	510	500	500	555	500	nd	nd	555	550	465
	Biomass flow rate (kg/h)	0.75	1	0.6	0.5	0.99	800 g db	900 g db	0.47	1	2–4
	Nitrogen flow rate (L/min)	nd	nd	20	6.9	36.7	3	3	6.9	nd	nd
Condensation system conditions	Nº condensers steps	4 stages	3 stages	3 stages	2 stages	2 stages	2 stages	2 stages	Scenario A: 2 stages Scenario B: 3 stages	3 Stages	2 stages
	Condensers temperature (°C)	Stage 1: 200 Stage 2: 150 Stage 3: - 5 stage 4: - 20	Stage 1: 170/130/100 Stage 2: 70 Stage 3: −10	Stage 1: 80 Stage 2: 25 Stage 3: 0	Stage 1: 120 Stage 2: 4	Stage 1: 85 stage 2: −10	Stage 1: 125–225 Stage 2: 25	Stage 1: 140–260 Stage 2 = 20	Scenario A: Stage 1: 120 Stage 2: 4 Scenario B: Stage 1: 180 Stage 2: 120 Stage 3: 4	Stage 1: 80 Stage 2: 70 Stage 3: 0	Stage 1: 90 Stage 2: 4
Efficiency parameters	Condensing efficiency	Stage 1–2: 0.07–0.22 Stage 3–4: 0.25–0.37 Total: 0.41–0.51	nd	nd	nd	nd	nd	nd	Scenario A: Stage 1: 0.17 Stage 2: 0.17 Total: 0.34 Scenario B: Stage 1: 0.15 Stage 2: 0.06 Stage 3: 0.24 Total:0.46	nd	nd
Liquid product	Total bio-oil yield ($kg_{bio-oil}/kg_{biomass\ db}$)	0.58–0.62	Average: 0.70	Average: 0.57	0.25	0.38	0.48	0.36	Scenario A: 0.24 Scenario B: 0.29	0.55	0.51
	Bio-oil yield (% wt. kg/kg bio-oil) per stage	Stage 1: 3.2–13.8 Stage 2:	Stage 1: 24.6 Stage 2: 18.6 Stage 3: 45.0	Stage 1:28.1 Stage 2 and 3	Stage 1: 41.7 Stage 2: 46.8	Stage 1: 35.7 Stage 2: 64.3	Stage 1: 62.5 Stage 2: 37.5	Stage 1: 63.9 Stage 2: 36.1	Scenario A: Stage 1: 42.5 Stage 2: 43.0	Stage 1: the rest	Stage 1: 37.3 Stage 2: 62.7

(*continued on next page*)

Table 1 (*continued*)

	Chai *et al.* [35]	Mati *et al.* [28]	Liaw *et al.* [37]	Álvarez-Chávez *et al.* [36]	Li *et al.* [38]	Le Roux *et al.* [39]	Le Roux *et al.* [39]	Álvarez-Chávez *et al.* [41]	Siriwardhana [32]	Papari *et al.* [42]
	3.2–17.2 Stage 3: 25.8–37.8 Stage 4: 9.7–34.4		(aqueous fraction): 38.6					Scenario B: Stage 1: 27.9 Stage 2: 13.9 Stage 3: 47.9	Stage 2: 62–65 Stage 3: 32–38	
Water concentration (% wt.)	Stage 1–2: 1.6–2.6 Stage 3: 53.6–65.1 Stage 4: 35.3–46.2	nd	Stage 1: 2.9 Aqueous fraction Stage 2 and 3 (aqueous fraction): 40.4	Stage 1: 16.86	Stage 1: 4.8 Stage 2: 64.8	Stage 1: 31 Stage 2: 65	Stage 1: 33 Stage 2: 76	Scenario 1: Stage 1: 14.59 Scenario 2: Stage 1: 11.15 Stage 2: 23.11	Stage1: < 2 Stage 2: 5 Stage 3: 62 Total - 38	Stage 1: 5.3 Stage 2: 34.4 (aqueous fraction and heavy fraction)
HHV (MJ/kg)	nd	Stage 1: 24–25 Stage 2: 21–22 Stage 3: 6–7	nd	Stage 1 = GHV 18.11	nd	nd	nd	Scenario 1: Stage 1: 17.57 Scenario 2: Stage 1: 18.87 Stage 2: 15.47	Stage 1: 31 Stage 2: 29 Stage 3: 5.5 Total - 17	Stage 1: 29 Stage 2: 12
pH	Stage 1–2: 6.1–6.6: Stage 3: 4.3–4.7 Stage 4: 4.2–4.6	nd	nd	Stage 1:2.6	Stage 1: 3.68 Stage 2: 2.24	Stage 1: 2.44 Stage 2: 2.19	Stage 1: 2.46 Stage 2: 2.56	Scenario 1: Stage 1: 2.61 Scenario 2: Stage 1: 2.56; Stage 2: 2.54	Stage 2: 2.5 Stage 3: 2.4 Total: 2.45	nd
Elemental analysis (kg i/kg bio-oil wb)	nd	Cond 1 a 170 °C: C: Stage 1:61.1 Stage 2: 53.4 H: Stage 1: 5.82 Stage 2: 6.60 N: Stage 1: 0.15 Stage 2: 0.55 Cond 1 a 130 °C: C: Stage 1:60.1 Stage 2: 51.7 H: Stage 1: 5.85 Stage 2: 6.63 N: Stage 1: 0.13 Stage 2: 0.59 Cond 1 a 100 °C: C: Stage 1:58.9 Stage 2: 53.0 H: Stage 1:6.10 Stage 2: 6.62 N: Stage 1: 0.31 Stage 2: 0.07	nd	nd	nd	nd	nd	nd	nd	nd
Empirical chemical formula	nd	Cond 1 a 170 °C Stage 1: $CH_{1.14}O_{0.40}N_{0.002}$	nd	nd	nd	nd	nd	nd	nd	nd

(*continued on next page*)

Table 1 (*continued*)

	Chai *et al.* [35]	Mati *et al.* [28]	Liaw *et al.* [37]	Álvarez-Chávez *et al.* [36]	Li *et al.* [38]	Le Roux *et al.* [39]	Le Roux *et al.* [39]	Álvarez-Chávez *et al.* [41]	Siriwardhana [32]	Papari *et al.* [42]
		Stage 2: $CH_{1.48}O_{0.55}N_{0.009}$ Cond 1 a 130 °C: Stage 1: $CH_{1.17}O_{0.42}N_{0.002}$ Stage 2: $CH_{1.54}O_{0.60}N_{0.01}$ Cond 1 a 100 °C: Stage 1: $CH_{1.24}O_{0.44}N_{0.005}$ Stage 2: $CH_{1.50}O_{0.57}N_{0.001}$								
Phenolic compounds (relative content %)	nd	nd	nd	Stage 1: 32	nd	Stage 1: 70.04 Stage 2: 51	Stage 1: 45.71 Stage 2: 43.95	Scenario 1: Stage 1: 33.47 Scenario 2: Stage 1: 38.93 Stage 2: 31.33	nd	Stage 1: detected Stage 2: detected in aqueous and heavy fractions
Furans (relative content %)	nd	nd	nd	nd	nd	Stage 1: 6.7 Stage 2: 16.58	Stage 1: 1.44 Stage 2: 6.54	nd	nd	Stage 1: detected Stage 2: detected in aqueous and heavy fractions
Anhydro sugars (relative content %)	nd	nd	nd	nd	nd	Stage 1: 6.35 Stage 2: 22.79	Stage 1: 1.54 Stage 2: 16.27	nd	nd	Stage 1: detected Stage 2: detected in aqueous and heavy fractions
Alcohol (relative content %)	nd	nd	nd	nd	nd	Stage 1: 0 Stage 2: 0	Stage 1: 25.6 Stage 2: 0	nd	nd	Stage 2: detected in aqueous fractions
Ketones (relative content %)	nd	nd	nd	Stage 1: 12.2	nd	Stage 1: 5.62 Stage 2: 5.82	Stage 1: 0 Stage 2: 2.95	nd	nd	Stage 2: detected in aqueous fraction
Acids (relative content %)	nd	nd	nd	Stage 1: 6.2	nd	nd	nd	Scenario 1 Stage 1: 7.67 Scenario 2: Stage 1: 4.23 Stage 2: 6.51	nd	Stage 2: detected in aqueous and heavy fractions

wb – wet basis; db – dry basis; M – Moisture; VM – Volatile matter; FC: Fixed carbon; nd – data not available

Fig. 1. Macroscopic appearance of the RBE types used in the pyrolysis experiments: (EB) *E. globulus* branches, (EL) *E. globulus* leaves.

Table 2
Proximate and ultimate analysis of the *E. globulus* branches and leaves used as feedstock in the pyrolysis experiments.

	EB	EL
Proximate analysis		
Moisture (%wt., wb)	8.68	8.80
Ash (%wt., db)	4.15	5.60
Volatile matter (%wt., db)	75.30	83.20
Fixed carbon (%wt., db)	20.55	11.20
Elemental analysis (%wt., db)		
C	50.27	53.71
H	6.33	7.01
N	0.80	1.25
O	38.45	32.42
LHV (MJ/kg db)	19.55	20.98
Empirical chemical formula	$CH_{1.51}O_{0.57}N_{0.01}$	$CH_{1.57}O_{0.45}N_{0.02}$

wb – wet basis; db – dry basis; EB – *E. globulus* branches; EL – *E. globulus* leaves

Stage 3 (S3) (as depicted in Fig. 2) electrically heated and a set of condensers, Stage 4 (S4) (impingers made of borosilicate) submerged in an ice bath at atmospheric pressure, or just a set of condensers submerged (single stage) in an ice bath at atmospheric pressure, respectively. The temperatures of the three stainless steel condensers are controlled using K type thermocouples and electric resistances, controlled in cascade mode by an electronic control system. After condensation, non-condensable gas (referred to as permanent gas and purge gas) is directed to an exhaust system and/or collected in a sampling bag for subsequent chromatographic analysis.

ii. Vapors burner: excess pyrolysis vapors are burnt before emission into the atmosphere.

2.2.2. Operating conditions

The operating conditions for the RBE pyrolysis experiments are presented in Table 3. The pyrolysis experiments were conducted at 550 °C, selected based on previous work by Vilas-Boas *et al.* [45], which identified this temperature as optimal for maximizing bio-oil production. To prevent atmospheric air (and thus O_2) from entering the reactive system, a nitrogen (N_2) purge was injected into both the biomass feed silo and the biochar discharge silo, with flow rates of 1.5 L_{NPT}/min and 1.0 L_{NPT}/min, respectively. Here, NPT refers to standard pressure (1.013×10^5 Pa) and temperature (273 K).

The temperatures of each condensation stage in the FCS were selected to maximize the separation of bio-oil fractions with low water concentration and distinct chemical compounds as a function of boiling point. These temperatures settings were chosen based on studies reported in the literature [22,29,46], the boiling points of compounds typically found in pyrolysis bio-oils [47], and preliminary experiments made by the authors.

In stage 1 (S1 in Fig. 2), the temperature was set at 140 °C to promote the preferential condensation of compounds with boiling points above 140 °C, such as high-molecular-weight compounds, particularly aromatic compounds, and other long-chain hydrocarbons, while minimizing water condensation. Preliminary experiments showed that higher temperatures (e.g.,180 °C) caused condensation of a very low mass fraction of high molecular weight compounds that solidified under further quenching at room temperature, making recovery challenging.

In stage 2 (S2 in Fig. 2), a temperature of 100 °C was used to condense aromatic compounds of lower molecular weight, including phenols, with boiling points in the range of 100–140 °C, while still limiting water condensation.

Stage 3 (S3 in Fig. 2) and stage 4 (S4 in Fig. 2) were designed to collect most of the water vapor and light oxygenated compounds. Stage 3, set at 60 °C, was chosen to collect light oxygenated compounds with lower concentration of water and organic acids, which are undesirable

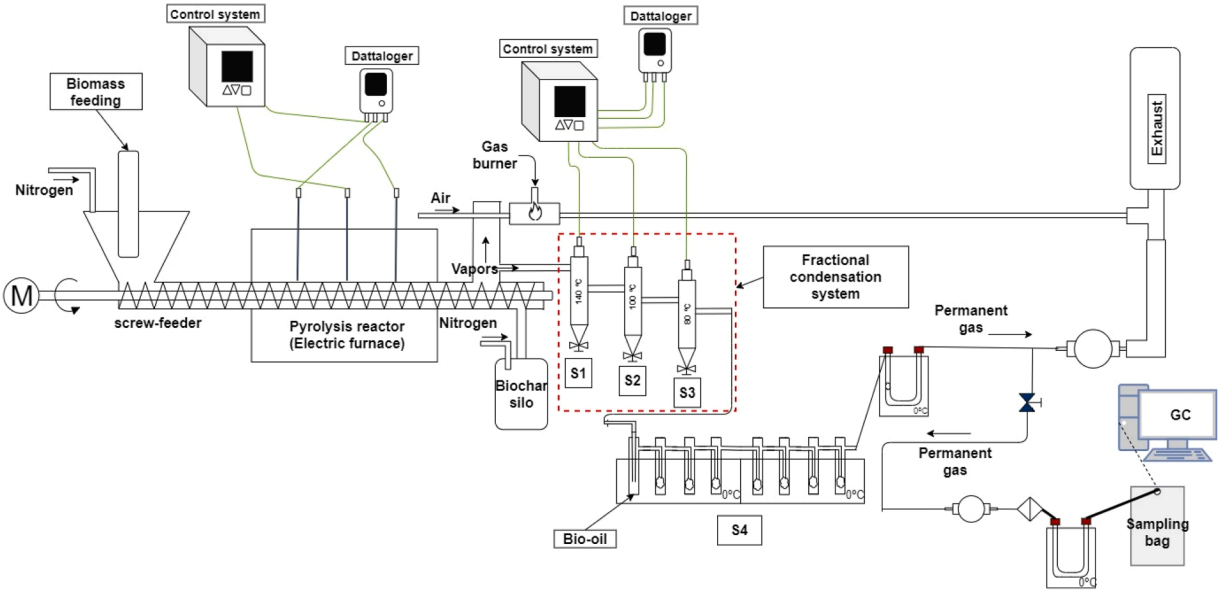

Fig. 2. Schematic representation of the experimental facility with a prototype-scale auger reactor for biomass pyrolysis studies and pyrolysis vapors condensation units. S1 – Stage 1, S2 – Stage 2, S3 – Stage 3; S4 – Stage 4.

Table 3
Operating conditions used in this study.

Reference of experiment		EB-FCS	EL-FCS	EL-SCS
Feedstock		EB	EL	
Pyrolysis temperature (°C)		550		
Biomass flow rate (kg/h)		0.47	0.28	0.52
Solids residence time at the pyrolysis temperature (min)		5		
N_2 flow (L_{NPT}/min)		2.5		
Operation time (h:min)		3h55min	5h32min	4h56min
Condensation system		FCS		SCS
Permanent gas flow after condensation system (L_{NPT}/min)		0.79	0.74	0.83
Residence time of gas in stainless steel condensers (min)		14.1	14.9	-
Temperature of condensation stages (°C)	S1	112–148 (140[a]; 127[b]; ± 8.6[c])	137–146 (140[a]; 140[b]; ± 1.7[c])	≈ 0 °C
	S2	89–124 (100[a]; 107[b]; ± 8.1[c])	90–109 (100[a]; 102[b]; ± 3.3[c])	
	S3	69–86 (80[a]; 76[b]; ± 4.3[c])	67–89 (80[a]; 73[b]; ± 3.4[c])	
	S4	≈ 0 °C		

NPT means standard pressure (1×10^5 Pa) and temperature (273 K), EB – E. *globulus* branches, EL – E. *globulus* leaves, FCS – Fractional condensation system, SCS – Single-stage condensation system. S1 – Stage 1, S2 – Stage 2, S3 – Stage 3; S4 – Stage 4.
[a] Desired temperature;
[b] Average;
[c] Standard deviation.

due to their contribution to bio-oil chemical instability [48]. Finally, stage 4, set at 0 °C, was used to condense the remaining vapors, consisting of water, and highly volatile and water-soluble compounds, such as light alcohols, short-chain carboxylic acids.

Despite the predefined temperatures, it was not always possible to maintain a stable temperature as desired. This occurred due to fluctuations in the biomass feed to the pyrolysis reactor and, consequently, in the vapors flow produced, as evidenced by the actual temperature ranges during the experiments shown in Table 2.

2.3. Condensation efficiency

The methodology adopted to assess efficiency of the FCS relative to the SCS was based on the approach presented by Wang *et al.* [49]. This efficiency is used as an indicator of the separation between the condensable (bio-oil) and the non-condensable (permanent gas) fractions and is calculated as a ratio between the yield of bio-oil collected in the condensers and the total yield of vapors formed during pyrolysis, according to Eq. (1).

$$\text{Condensation efficiency} = \frac{\dot{m}_{BO}}{\dot{m}_{BM,wb} - \dot{m}_{BC}} \quad (1)$$

Where $\dot{m}_{BO}$ represents the total mass flow rate (kg/h) of bio-oil collect in the condensers, $\dot{m}_{BM,wb}$ corresponds to the mass flow rate (kg/h) of fed biomass (wb), and $\dot{m}_{BC}$ is the mass flow rate (kg/h) of biochar produced during pyrolysis experiment.

2.4. Products yields and bio-oil distribution

During the experiments, various parameters were recorded, including the mass flow rate of fed biomass ($\dot{m}_{BM,wb}$, kg/h), the purge N_2 flow rate (L_{NPT}/min), the mass flow rate of biochar ($\dot{m}_{BC}$, kg/h), the total mass flow rate of bio-oil collected in the condensation systems ($\dot{m}_{BO_2}$, kg/h), the gas (permanent gas and purge N_2) flow rate downstream (V_{G_2}, Nm^3/h) the condensation system.

Based on this data and the diagram shown in Fig. 3, the mass balance of the pyrolysis system was performed to determine the product's yield, according to Eq. 2:

$$\dot{m}_{BM,wb}(\text{kg/h, wb}) = \dot{m}_{V_1}(\text{kg/h}) + \dot{m}_{V_2}(\text{kg/h}) + \quad \dot{m}_{BC}(\text{kg/h}) \quad (2)$$

Where, $\dot{m}_{V_1}$ and $\dot{m}_{V_2}$ are the mass flow rates of pyrolysis vapors in stream 1 and stream 2, respectively, in kg/h, according to Eqs. 3 and 4.

$$\dot{m}_{V_1}(\text{kg/h}) = \quad \dot{m}_{PG_1}(\text{kg/h}) + \quad \dot{m}_{BO_1} \quad (\text{kg/h}) \quad (3)$$

$$\dot{m}_{V_2}(\text{kg/h}) = \quad \dot{m}_{BO_2}(\text{kg/h}) + \dot{m}_{PG_2}(\text{kg/h}) \quad (4)$$

Where, $\dot{m}_{PG_1}$ and $\dot{m}_{BO_1}$ are the mass flow rates of vapor precursors of permanent gas and bio-oil in stream 1, respectively, which are sent directly to the combustion chamber. $\dot{m}_{PG_2}$ and $\dot{m}_{BO_2}$ are the mass flow rate of vapor precursors of permanent gas and bio-oil in stream 2, respectively, that passes through the condensation system, corresponding to the permanent gas and bio-oil collected in the condensation system.

The mass flow rate of permanent gas in stream 2 ($\dot{m}_{PG_2}$) was determined using the ideal gas behavior approach (Eq. 5), for a pressure of 1.013×10^5 Pa and temperature of 298 K. The molar mass of the permanent gas at the condensation system exit (M_{PG2}, kg/kmol) was calculated based on its composition, as determined by gas chromatography.

$$\dot{m}_{PG_2}(\text{kg/h}) = \frac{\dot{V}_{PG_2}(\text{Nm}^3/\text{h}) \bullet P(\text{Pa}) \bullet M_{PG_2}\left(\frac{\text{kg}}{\text{kmol}}\right)}{R\left(\frac{\text{Nm}^3 \bullet \text{Pa}}{\text{K} \bullet \text{kmol}}\right) \bullet T(\text{K})} \quad (5)$$

The volume flow rate of the permanent gas in stream 2 ($\dot{V}_{PG_2}$) was calculated based on the measured total gas volume flow rate ($\dot{V}_{G_2}$) at the condensation system exit and the volumetric fraction of the permanent gas in the total measured gas (N_2 + permanent gas), as given by Eq. 6.

$$\dot{V}_{PG_2}(\text{Nm}^3/\text{h}) = \quad \dot{V}_{G_2}(\text{Nm}^3/\text{h}) \bullet y_{GG_2}(\text{Nm}^3_{PG2}/\text{Nm}^3_{G2}) \quad (6)$$

The total yield of bio-oil and permanent gas was determined as the sum of precursors vapors of permanent gas and bio-oil yield in stream 1 ($\eta_{PG_1-V_1}$ and $\eta_{BO_1-V_1}$) and permanent gas and bio-oil in stream 2 ($\eta_{PG_2-V_2}$ and $\eta_{BO_2-V_2}$), respectively. Since pyrolysis vapor streams 1 and 2 originate from the main pyrolysis vapor stream, the assumptions given by Eqs. 7 and 8 were considered.

$$\eta_{BO_1-V_1}(\%) = \quad \eta_{BO_2-V_2} \quad (\%) \quad (7)$$

$$\eta_{PG_1-V_1}(\%) = \quad \eta_{PG_2-V_2} \quad (\%) \quad (8)$$

Where $\eta_{BO_1-V_1}$ and $\eta_{BO_2-V_2}$ were calculated according to Eqs. 9 and 10:

$$\eta_{BO_1-V_1}(\%) = \quad \frac{\dot{m}_{BO_1}(\text{kg/h})}{\dot{m}_{V_1}(\text{kg/h})} \times 100 \quad (9)$$

$$\eta_{BO_2-V_2}(\%) = \quad \frac{\dot{m}_{BO_2}(\text{kg/h})}{\dot{m}_{V_2}(\text{kg/h})} \times 100 \quad (10)$$

The total yield of bio-oil (η_{BO_T}, %wt., $kg_{\text{bio-oil as collect}}/kg_{\text{biomass db}}$) was calculated using Eq. 11.

$$\eta_{BO_T}(\%) = \quad \frac{\dot{m}_{BO_1}(\text{kg/h}) + \dot{m}_{BO_2}(\text{kg/h})}{\dot{m}_{BM,db}(\text{kg/h})} \times 100 \quad (11)$$

The yields of permanent gas $\eta_{PG_1-V_1}$ and $\eta_{PG_2-V_2}$ were calculated using Eqs. 12 and 13.

$$\eta_{PG_1-V_1}(\%) = \quad \frac{\dot{m}_{PG_1}(\text{kg/h})}{\dot{m}_{V_1}(\text{kg/h})} \times 100 \quad (12)$$

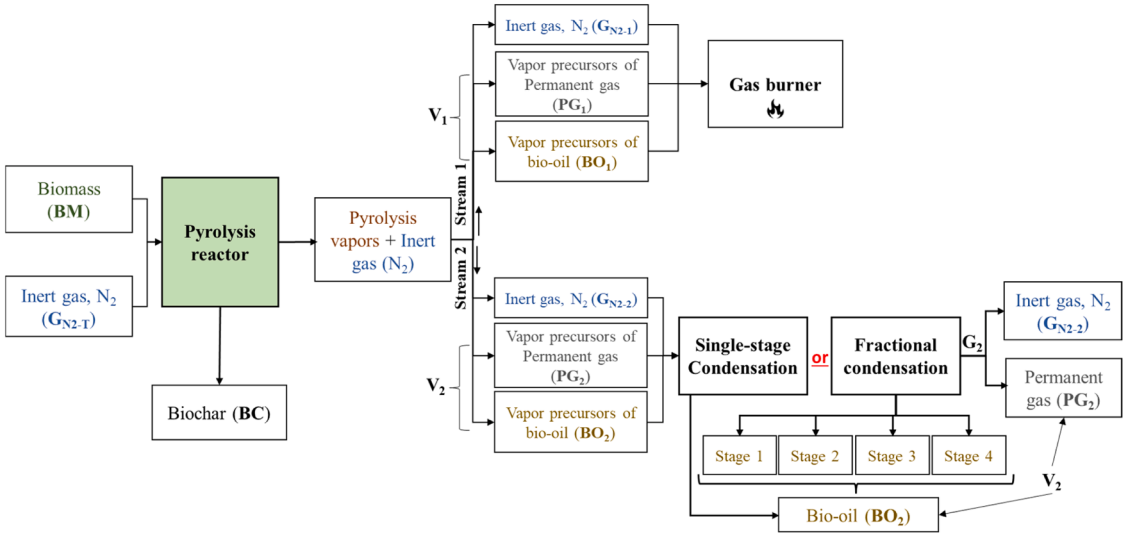

Fig. 3. Schematic diagram used for mass balance of the pyrolysis experiments conducted in this study.

$$\eta_{PG_2-V_2}(\%) = \frac{\dot{m}_{PG_2}(\mathrm{kg/h})}{\dot{m}_{V_2}(\mathrm{kg/h})} \times 100 \quad (13)$$

The total permanent gas yield (η_{PG}) and biochar yield (η_{BC}) were determined using Eq. 14 and Eq. 15, respectively.

$$\eta_{PG}\left(\%, \frac{\text{kg gas/h}}{\text{kg biomass, db/h}}\right) = \frac{\dot{m}_{PG_1}(\mathrm{kg/h}) + \dot{m}_{PG_2}(\mathrm{kg/h})}{\dot{m}_{BM,db} \quad (\mathrm{kg/h})} \times 100 \quad (14)$$

$$\eta_{BC}\left(\%, \frac{\text{kg biochar/h}}{\text{kg biomass, db/h}}\right) = \frac{\dot{m}_{BC} \quad (\mathrm{kg/h})}{\dot{m}_{BM,db} \quad (\mathrm{kg/h})} \times 100 \quad (15)$$

In the fractional condensation system, the distribution of bio-oil across the different stages was calculated based on the mass of bio-oil collected at each stage, following the same calculation model.

2.5. Characterization of bio-oil

In the SCS, the collected bio-oil naturally separated into two distinct fractions after condensation. These were separated by decantation and labeled according to their density as the heavy fraction (HF-SCS) and light fraction (LF-SCS). Similarly, in the fractional condensation system, the bio-oil collected at different stages also separated into two fractions immediately after collection, which were similarly decanted and labeled as HF-FCS and LF-FCS. The exception was the bio-oil sample collected in stage 1, which only presented a fraction similar to the heavy fraction and was therefore labeled as HF-FCS.

In general, compared to the LF, the HF of the bio-oil collected at all condensation stages, both in FCS and SCS, exhibited a dark color, homogeneous appearance, and high viscosity properties. However, as the temperature decreased in FCS, a reduction in the viscosity of the bio-oil HF was observed. The HF-FCS from stage S4 presented an appearance similar to that of HF-SCS. The LF of the bio-oil at all condensation stages, both in FCS and SCS, showed a lighter color, lower viscosity and density. Additionally, as the condensation temperature decreased in FCS, the LF bio-oil showed changed in color, becoming lighter at lower temperatures. In most of the fractional condensation studies reported in the literature, the separation of bio-oil into two distinct fractions in the condensation stages immediately after collection is not mentioned. These studies typically only refer to the presence of more aqueous fractions at lower temperatures.

After pyrolysis experiments and bio-oils being processed by decantation, the samples were stored in closed glass containers at approximately −13 ºC. All bio-oil fractions were further characterized for their water concentration using volumetric Karl Fischer titration (SI Analytics Automatic Titrator TitroLine 7500) and volatile organic composition identification by gas chromatography-mass spectrometry (GC-MS). An Agilent 8890 GC, equipped with an Agilent DB-5ms 30 m x 250 μm x 0.25 μm column, was used, coupled with an Agilent 5977B GC/MSD (Mass Spectrometer). The HF samples were prepared by dissolving around 5 mg of HF bio-oil in 0.5 mL of hexane, while the LF samples were injected into the GC without solvent dilution. A volume of 0.1 μL was used for the GC analysis. The column flow was 1 mL/min, with helium as the carrier gas, and the split ratio was 10:1 for HF samples and 400:1 for LF bio-oil samples. The inlet pressure 8.2 psi, and the inlet temperature was set to 250 °C. The oven temperature program started at 60 °C, ramping at 15 °C/min up to 100 °C, followed by 25 °C/min up to 260 °C with a 15 min hold time, and then 25 °C/min up to 300 °C with a 5 min hold time. The MS transfer line temperature was 250 °C, the MS source temperature was 230 °C, and the MS quadrupole temperature was 150 °C. MS scan time segments were as follows: 0 min (start mass 10, end mass 250), 7 min (start mass 40, end mass 340), both with a scan speed of 781. The chromatographic peaks were identified using NIST 17.

It is important to note that while GC-MS is widely applied for bio-oil analysis due to its ability to identify various compounds, this technique is limited to detecting primarily volatile and semi-volatile compounds, representing approximately 30 %wt. of the total compounds present in pyrolysis bio-oil [22,50]. Therefore, the compounds identified correspond only to the detectable fraction within the range of this technique.

Additionally, the HF fractions were submitted for elemental composition analysis (C, H, N, following ASTM D 5291 standard), with oxygen concentration calculated by difference, and higher heating value (HHV) was determined using an oxygen bomb calorimeter according to ASTM D240.

3. Results and discussion

3.1. Condensation efficiency

The condensation efficiency of the FCS was similar to that of the SCS used in this work, with values of approximately 0.62 and 0.61, respectively. These values are slightly higher than those reported in the literature, which range between 0.34 and 0.51 [35,51]. This difference may be attributed to variations in the configuration and operating temperatures of the condensation system, as well as the type of biomass used, which influences the composition of the vapors formed during the pyrolysis reactions and respective liquid fraction obtained.

Regarding the condensation efficiency at each stage of the FCS, an increasing trend was observed with decreasing condensation temperature (Fig. 4), except in the second stage. This deviation can be attributed to the proximity between the condensation temperatures of the first and second stages, a phenomenon observed more prominently in the pyrolysis experiments of *E. globulus* branches. This suggests the need for optimization of the condensation temperatures in these two stages. Additionally, condensation efficiency was significantly higher in the third and fourth stages, where lower temperatures favored the condensation of a greater amount of water, as further analyzed in Section 3.3.

3.2. Yields of products and fractional bio-oil distribution

The yields of pyrolysis products and the distribution of bio-oil, including the HF and LF, across the different stages of fractional condensation are presented in Fig. 5. The product yields were calculated based on the mass of product generated per kilogram of dry biomass processed (Eqs. 11, 14 and 15 in Section 2.4). The total bio-oil yield includes all the condensable vapors produced during pyrolysis, including the water generated by the process reactions and the original moisture content of the biomass.

The product yields were similar for both types of biomass, with biochar yield ranging from 0.28 to 0.30 $kg_{biochar}/kg_{dry\ biomass}$, bio-oil yield ranging from 0.48 to 0.49 $kg_{bio\text{-}oil}/kg_{dry\ biomass}$, and permanent gas yield ranging from 0.31 to 0.33 $kg_{permanent\ gas}/kg_{dry\ biomass}$ (Fig. 5a). No significant differences were observed in total bio-oil yield between the SCS and the FCS (Fig. 5a). Furthermore, bio-oil yields were consistent across different types of biomass residues, ranging from 0.47 to 0.49 $kg_{biochar}/kg_{dry\ biomass}$, in agreement with values reported in the literature (Table 1).

Regarding the distribution of bio-oil yield across the condensation stages, the highest yields were observed in stages with temperatures below 100 °C (stages 3 and 4), attributed to the high-water concentration in the bio-oil, ranging from 76.5 % to 84.6 %wt. of the total bio-oil collected. The remaining bio-oil was collected in the first and second stages, accounting for values in the range 15.1–23.6 %wt. of the total. In stage 2, bio-oil collection was minimal, particularly during the pyrolysis of *E. globulus* branches, with a yield of around 3.2 %wt., suggesting the possibility of eliminating this stage or optimizing the temperatures in stages 1 and 2. Compared to data from the literature for condensers operating at temperatures above 100 °C, the yields observed in this study were lower (Table 1). This difference may be related to specific process conditions, such as the use of dry biomass and its physicochemical characteristics, as well as the configuration of the condensation system, which may influence the residence time of the pyrolysis vapors.

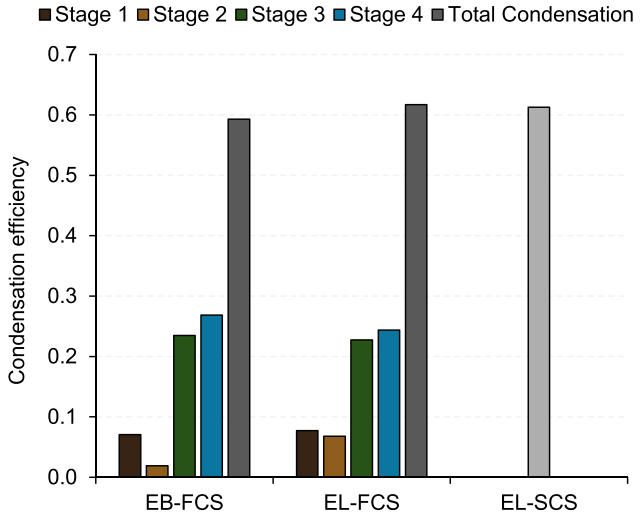

Fig. 4. Condensation efficiency of the fractional and single-stage condensation systems for pyrolysis vapors from *E. globulus* branches and leaves. Total condensation represents the sum of the condensation efficiency of stages 1, 2, 3, and 4.

As described in the methodology (Section 2), the bio-oil collected in both condensation systems spontaneously separated into two distinct fractions. The exception was observed for the bio-oil collected in stage 1, which consisted of a single fraction, possibly due to its low water concentration, as the condensation temperature exceeded 100 °C. It is frequently reported in the literature (Table 1) that organic-rich fractions are typically condensed at higher temperatures while more aqueous fractions are collected at lower temperatures. However, this study demonstrated that phase separation into heavy and light fractions can occur across multiple condensation stages, including intermediate and low-temperature stages. This observation underscores the complexity of bio-oil behavior, which varies with feedstocks characteristics, condensation technologies, and operating conditions. These findings highlight the importance of studying fractionation behavior under realistic process conditions to better understand the mechanisms governing bio-oil phase separation.

The HF and LF fractions were quantified, and their distribution is shown in Fig. 5c. The total yields of HF and LF were similar for both systems. Comparing the pyrolysis experiments of *E. globulus* residues in the FCS, it was noted that the pyrolysis of *E. globulus* leaves resulted in a slightly higher proportion of HF, which may be relevant for its application as a fuel. However, a detailed analysis of its physicochemical properties, including water concentration, elemental composition, and other characteristics, will be discussed in Sections 3.3–3.6.

Approximately 40 %wt. of HF was collected in the first condensation stage in both experiments, likely consisting mainly of long-chain compounds, primarily lignin-derived compounds and some sugars. However, small amounts of these compounds might also be transported to subsequent condensation stages [42,47]. In contrast, over 90 %wt. of the LF was collected in the stages with temperatures below 100°C (stages 3 and 4), primarily composed of water and water-soluble compounds, as will be analyzed in Sections 3.3, 3.4 and 3.6.

3.3. Water concentration in fractional bio-oil

Fig. 6 shows the water concentration (%wt., $kg_{water}/kg_{bio\text{-}oil}$) in the different bio-oil fractions (HF and LF) obtained at each condensation stage of the FCS and in the SCS. The water present in the bio-oil came from the moisture in the raw biomass and as a by-product of the dehydration reactions of hemicellulose, cellulose, and lignin during the pyrolysis process [52].

Although similar amounts of HF were collected in both FCS and SCS, notable differences were observed in their water concentration. The total water concentration in the HF from the FCS was significantly lower (16.1 %wt.) compared to that from the SCS (30.4 %wt.), as shown in Fig. 6. For the FCS, this overall value was calculated as a weighted average, based on the mass contribution of each individual HF fraction collected at different condensation stages and their corresponding water concentration. This approach allowed a direct and meaningful comparison with the single HF phase recovered from the SCS.

The higher concentration of organic compounds in the HF from the FCS compared to the SCS (Fig. 7) makes the first more promising for co-processing in conventional oil refineries. This characteristic facilitates the production of liquid fuels, which is of growing interest for integrating biofuels into conventional refining chains. Additionally, when analyzing each condensation stage individually, the HFs collected in the first three stages of EL pyrolysis vapors showed lower water concentration than the HF collected in the SCS. The water concentration in the HFs collected in the first three stages of FCS were 2.6 %wt., 20.6 %wt., and 15.2 %wt., respectively, representing reductions of 91 %, 30 %, and

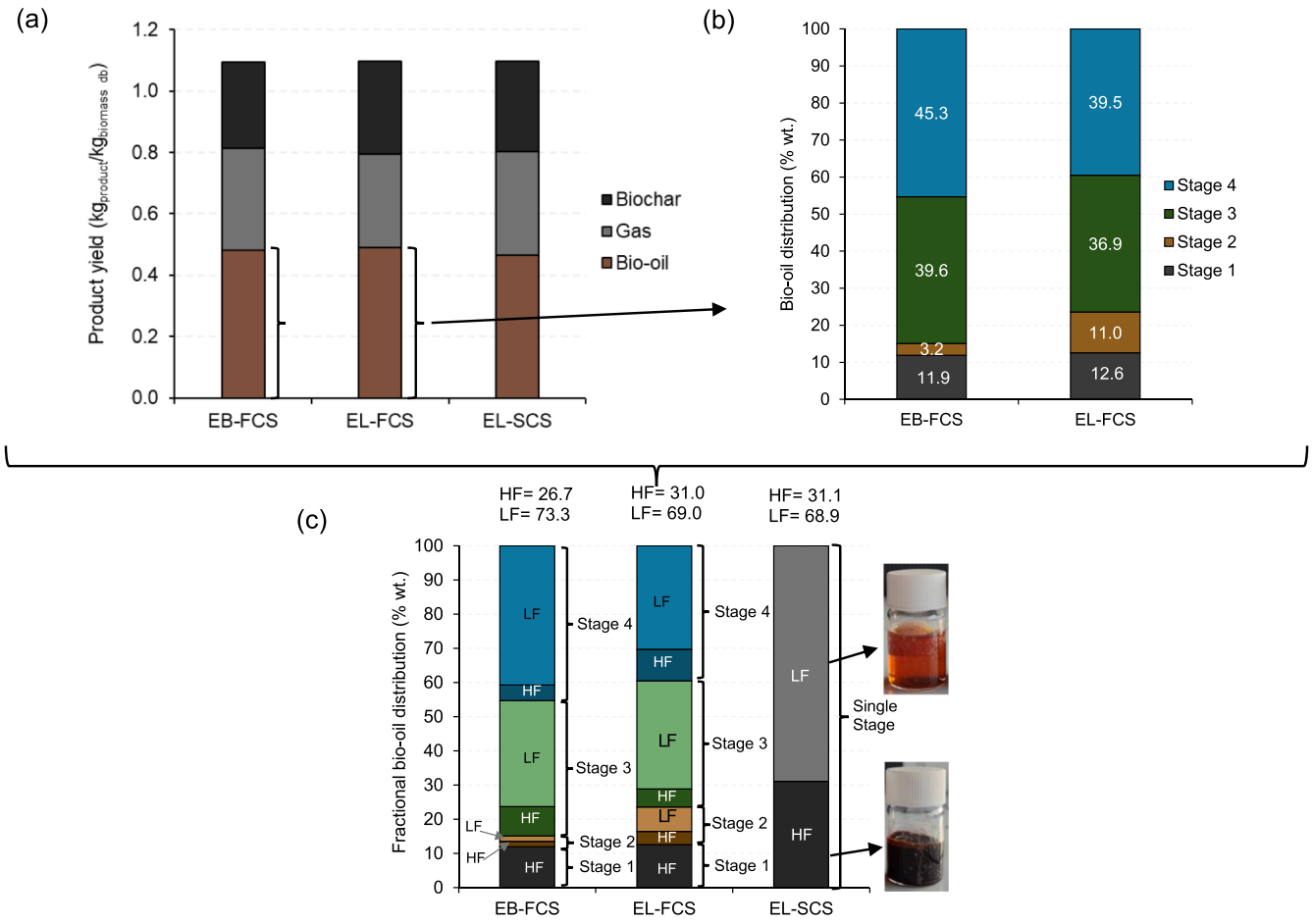

Fig. 5. Product yields and the distribution of bio-oil fractions (heavy and light fractions) at each stage (stage 1–4) of the fractional condensation system and in the single-stage condensation system, from *E. globulus* branches and leaves pyrolysis.

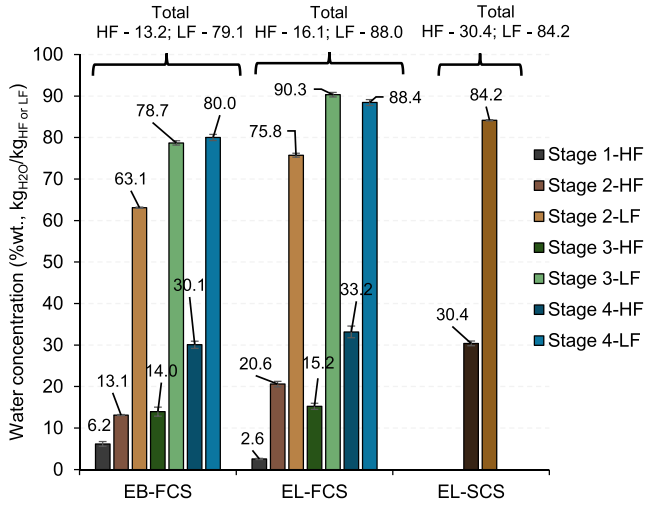

Fig. 6. Water concentration of heavy fraction and light fraction of bio-oil collected in fractional condensation system (stage 1–4) and in single-stage condensation system, from *E. globulus* leaves and branches pyrolysis.

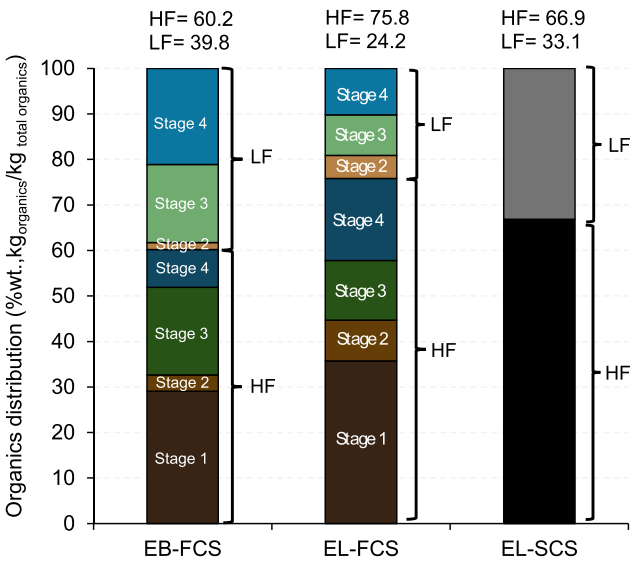

Fig. 7. Organic compounds concentration in heavy fraction and light fraction of bio-oil collected in fractional condensation system (stage 1–4) and in single-stage condensation system, from *E. globulus* leaves and branches pyrolysis.

49 %, respectively, compared to the water concentration in the HF collected in the SCS.

When comparing the pyrolysis experiments of EL and of EB using the FCS, a lower total water concentration was observed in both fractions (Fig. 6), HF and LF, collected in the experimental pyrolysis trial of *E.*

globulus branches. This result is counterintuitive, as EL had a lower oxygen concentration (see Table 2). However, other physicochemical properties of the biomass can influence the water formation. EL also has a higher volatile matter concentration and a lower fixed carbon concentration, which may result in greater production of volatile oxygenated compounds, facilitating dehydration and reactions and consequently increasing the water concentration in the bio-oil. Nevertheless, further studies are needed to fully understand the mechanisms involved.

It is important to highlight that the water concentration in the HFs collected in the first three stages for both EB and EL experiments, are within the water concentration limits (30 %wt.) established by the ASTM D7544–23 standard for the use of bio-oil in commercial or industrial burners adapted for liquid pyrolysis biofuels.

The high water concentrations in the LFs, ranging from 63.1 %wt. to 90.3 %wt., lead to the separation of the bio-oil into distinct fractions (HF and LF) [53], with the lowest water concentration values recorded in the LF of stage 2. The high-water concentrations indicate that the combustion of the LFs for thermal energy generation will be inappropriate.

3.4. Elemental analysis of heavy fractions of bio-oil

Fig. 8 presents the elemental analysis of the HFs of raw bio-oil, including water (wb), collected at different condensation stages in the FCS and the raw bio-oil from the SCS.

In the FCS, a general trend of increasing oxygen concentration and decreasing carbon concentration was observed from stage 1 to stage 4, though no clear tread was evident between stage 2 and stage 3. The HF from stage 1 showed the highest carbon concentration and the lowest oxygen concentration, primarily due to its lower water concentration. This characteristic makes it particularly interesting for co-processing in refineries, as the reduced water concentration facilitates processing and conversion into liquid fuels. Conversely, the HF from stage 4, despite its higher water concentration, contained fewer and less complex oxygenated compounds, also making it a promising candidate for refinery integration. Compared to literature data on fractional condensation of pyrolysis vapors (Table 1), the HF from stage 1 exhibited a higher carbon concentration at similar condensation temperatures, which may be related to operational conditions, such as a lower carbon concentration in the biomass used in the reference studies [28] compared to the biomass used in this work. Nevertheless, a general trend of decreasing carbon concentration in the bio-oil fractions collected along the stages is observed, that is, from condensation at higher temperature to lower temperature.

Based on the elemental analysis, the empirical chemical formulas of the bio-oils HFs collected at different condensation stages of the FCS and the one collected in the SCS were determined and are presented in

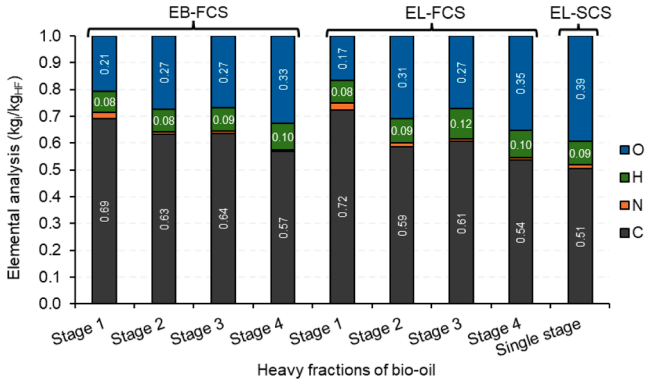

Fig. 8. Elemental composition in different heavy fractions of raw bio-oil (wb) collected in fractional condensation system (stage 1–4) and in single-stage condensation system, from *E. globulus* leaves and branches pyrolysis.

Table 4
Empirical chemical formulas of the heavy fractions of bio-oil collected in the fractional condensation system (stage 1–4) and in the single-stage condensation system, as well as for the original biomass, on a dry basis, from *E. globulus* branches and leaves.

Condensation system	Heavy fraction of bio-oil samples	EB	EL
FCS	Stage 1	$CH_{1.23}O_{0.16}N_{0.03}$	$CH_{1.35}O_{0.15}N_{0.03}$
	Stage 2	$CH_{1.32}O_{0.19}N_{0.01}$	$CH_{1.42}O_{0.31}N_{0.02}$
	Stage 3	$CH_{1.35}O_{0.17}N_{0.01}$	$CH_{1.94}O_{0.17}N_{0.01}$
	Stage 4	$CH_{1.38}O_{0.08}N_{0.01}$	$CH_{1.46}O_{0.08}N_{0.01}$
SCS	Single Stage	-	$CH_{1.31}O_{0.19}N_{0.02}$
Original Biomass		$CH_{1.51}O_{0.57}N_{0.01}$	$CH_{1.57}O_{0.45}N_{0.02}$

Table 4 (dry basis). The HF collected in the SCS showed an intermediate elemental composition (molar basis) compared to the fractions from the FCS. Although no clear trend is observed in the elemental composition across the FCS stages, the HF from stage 4 presented a lower O/C molar ratio and a higher H/C molar ratio, suggesting a reduction in oxygenated and aromatic compounds and an increase in aliphatic compounds. In contrast, the HF from stage 1 exhibited a lower H/C ratio, indicating the predominance of complex aromatic structures, typical of the initial lignin degradation during pyrolysis.

3.5. Heating value of heavy fractions of bio-oil

Fig. 9 depicts the heating value of each HF of bio-oil collected at different condensation stages of the FCS and in the single-stage of SCS. The figure presents the HHV of raw HF bio-oil (wb) as determined by calorimetric bomb, the corresponding LHV (wb) calculated for the raw HF, and the LHV on a dry basis, which excludes bio-oil water concentration.

All HFs of bio-oil exceeded the minimum value of LHV (wb) 15.0 MJ/kg established by ASTM D7544–23 for use in commercial or industrial burners adapted for liquid pyrolysis biofuels, with values ranging from 21.4 to 31.3 MJ/kg (wb). These values surpass the LHV of the original biomass Table 2. The HF collected at any stage of the FCS exhibited higher heating value than those collected in the SCS, particularly in the first three condensation stages. This behavior is attributed to the lower water and oxygen concentrations, along with an increased carbon concentration, which together enhances the energy density of these bio-oil fractions. Additionally, the water concentration in the HFs of bio-oil collected in the first three stages fell within the limits established by the ASTM D7544–23 standard, as detailed in Section 3.3. These results highlight the potential of these HFs of bio-oil for fuel applications in compliance with ASTM D7544–23. However, further analyses, including solids concentration, kinematic viscosity at 40 °C, and density at 20 °C are needed to fully assess their suitability.

Furthermore, the HHV of the bio-oil collected in stage 1 exceeds values reported in the literature for similar condensation temperatures using pine wood [28]. Although other studies have also obtained bio-oil fractions with comparable HHV, this was generally achieved using lower condensation temperatures and different types of biomass, such as dry birch bark and fresh softwood sawdust [32,42].

3.6. Chemical composition of bio-oil

Fig. 10 and Fig. 11 present the relative area percentages of chemical groups identified in the HF and LF bio-oil fractions collected in FCS and SFC. These area percentages were determined by GC-MS, meaning that the identified compounds correspond only to a detectable fraction within the range of this technique, as already mentioned in Section 2.5. Detailed data on the identified compounds and their respective area percentages within each chemical group for both fractions are provided in Supplementary Tables S1 and Table S2. The total area percentage of the identified compounds ranged from 44 % to 78 % in the HF samples

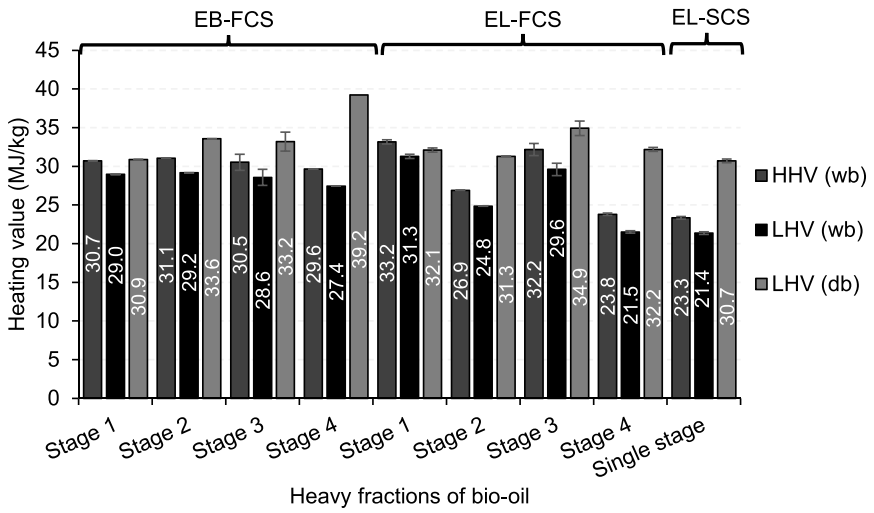

Fig. 9. Heating value of heavy fractions of bio-oil collected in the fractional condensation system (stage 1–4) and the single-stage condensation system, from *E. globulus* leaves and branches pyrolysis. Note: Error bars are included in data but have a low amplitude that in some cases makes it almost not visible, reflecting the high reproducibility of the measurements.

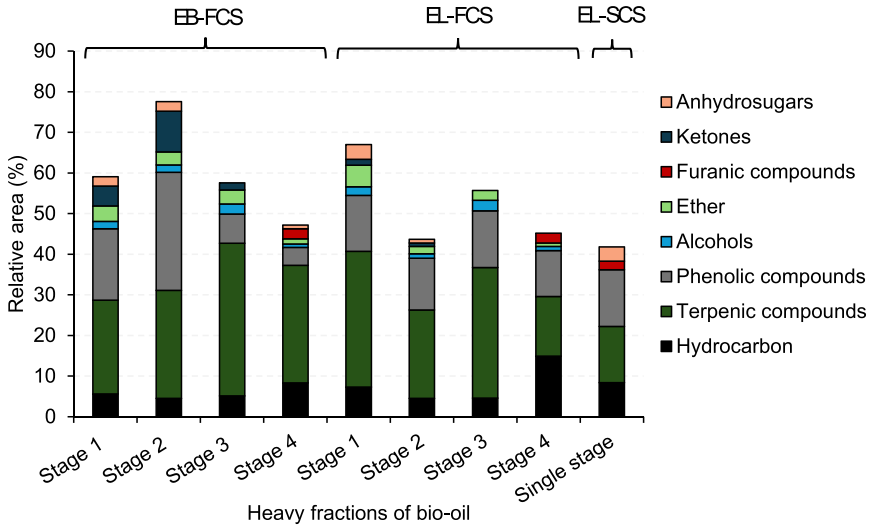

Fig. 10. Relative area percentage of chemical groups present in the heavy fraction of bio-oil collected in the fractional condensation system (stage 1–4) and the single-stage condensation system, from the pyrolysis of *E. globulus* branches and eucalyptus leaves.

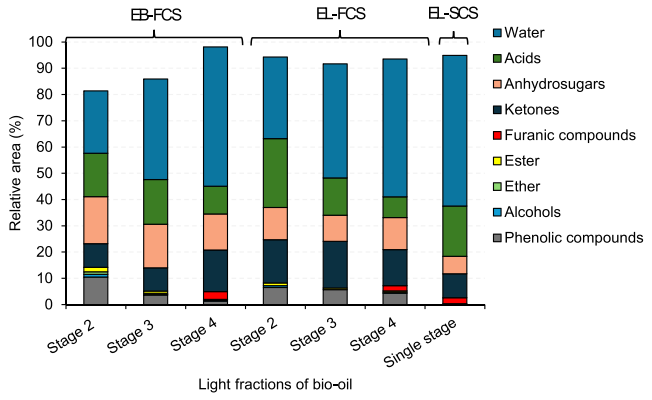

Fig. 11. Relative area percentage of chemical groups present in the light fractions of bio-oil collected in the fractional condensation system (stage 1–4) and the single-stage condensation system, from the pyrolysis of *E. globulus* branches and *E. globulus* leaves.

and from 81 % to 98 % in the LF samples. The identified compounds are categorized into different chemical groups: hydrocarbons, terpenic compounds, phenolic compounds, alcohols, ethers, esters, ketones, acids, furanic compounds, anhydrosugars, and other compounds.

In the HF of bio-oil collected from the SCS, phenolic compounds – mainly derived from lignin – were the dominant group, accounting for approximately 14 % of the total area. Within this group, phenol (3.9 %) and p-cresol (4.0 %) had the highest area percentages. The compound with the largest individual area percentage was aromadendrene, a sesquiterpene from *E. globulus* essential oil, representing 8.8 % of the total area. While *E. globulus* leaves typically yielded essential oils between 1.5 % and 2.7 %wt. after hydrodistillation [54]. Since pyrolysis is conducted at higher temperatures, the yield of essential oils may be slightly higher. However, given that the leaves used in this study had already undergone prior essential oil extraction, the high abundance of these compounds in the HF of the bio-oil collected from pyrolysis of *E. globulus* leaves was unexpected. This suggests that the identified compounds in Table S1 likely represent only a little fraction of the total composition, with additional unidentified compounds potentially

present in significant quantities.

For HF of bio-oil samples from FCS, terpenic and phenolic compounds were also the predominant groups in most condensation stages. However, hydrocarbons became more prevalent in HF from stage 4 for both biomass types, consisting mainly of lower molecular weight hydrocarbons compared to those detected in earlier stages.

Regarding the LF of bio-oil from SCS, the main groups identified were acids, ketones, and anhydrosugars, with total area percentages of 19.1 %, 9.1 %, and 6.7 %, respectively. These compounds are typical of polysaccharide (hemicellulose and cellulose) pyrolysis [47]. Acids were detected exclusively in this fraction, which can be explained by their high polarity and water solubility, properties compatible with the LF, which is richer in water, as discussed in Section 3.3. The relatively low percentage of phenolic compounds in this fraction, compared to literature data [55–58], may be attributed to differences in sample preparation (e.g., extraction methods or derivatization techniques) or the peak masking in the GC-MS chromatogram by more abundant compounds such as those of acetic acid or water.

Among the identified compounds with the highest area percentages in the LF of bio-oil from SCS, acetic acid (17.2 %) and levoglucosan (4.6 %) were prominent. Acetic acid, primarily formed during hemicellulose thermal degradation, has commercial value as a chemical feedstock [59]. Levoglucosan, the primary derivative of cellulose pyrolysis [60], is valuable in pharmaceuticals and polymers production [59,60], highlighting its potential for valorization. However, to make its separation and commercialization economically feasible, its concentration must be sufficiently high [61]. Still, the high relative abundance of these compounds suggests opportunities for direct use of the LF in biological processes, such as a substrate for anaerobic digestion, where sugars and acids are converted into biogas [37], or in agricultural applications, such as biological control agents (pesticides/herbicides) [57, 58,62]. In these fields, the high water concentration of the LF fraction can be an advantage. In anaerobic digestion, the dilution of organic compounds helps reduce toxicity to the microorganisms involved. In agricultural applications, it may facilitate use, for instance, in liquid spray formulations. Nevertheless, toxicity tests are essential to validate these applications. Alternatively, the LF could also be used for hydrogen production via reforming [63], which could, in turn, be used in upgrading steps of the HF of bio-oil to produce biofuels [63]. However, the presence of certain compounds, such as acetic acid itself, may pose technical challenges [64].

In the FCS, the LFs of bio-oils were collected in stages 2, 3, and 4, although stage 2 exhibited a relatively low percentage of this bio-oil fraction. The main compound groups in these fractions were, in most cases, anhydrosugars, acids, ketones, and phenolic compounds. For *E. globulus* branches, the compounds with the highest area percentages were acetic acid and levoglucosan across all three stages 2, 3 and 4. In the case of *E. globulus* leaves, acetone and acetic acid were the most abundant compounds in stages 2 and 3, while levoglucosan and acetic acid were predominant in stage 4.

Comparison between LFs from the FCS and SCS reveals that stage 4 of the FCS shows a lower percentage of total area of acidic compounds (notably acetic acid), which could contribute to reduced bio-oil acidity in this fraction, indicating the potential of the FCS for partial separation of this group. Additionally, furans, such as furfural, were exclusively found in stage 4 of the FCS (in both HF and LF), indicating partial separation of this compounds group. According to the literature, furans can also be detected in higher temperature condensation stages, but they are most abundant in lower temperature condensation stages [39]. Furthermore, a lower phenol content was also observed in stage 4 (at 0 ºC), which is consistent with the literature [39,41].

Nonetheless, fractionated condensation did not achieve a clear separation of different compound groups. This may be due to the influence of intermolecular interactions in the pyrolysis vapors rather than solely boiling points, leading to the formation of azeotropic mixtures [22]. For example, sugar derivatives, despite their high boiling points, were not exclusively retained in stage 1 of the FCS. Instead, these compounds were distributed across stages 1 and 2 in HF, and across stages 2, 3, and 4 in the LF, with a higher relative content in the LF. Phenolic compounds, in turn, were predominantly retained in the initial stages: stages 1 and 2 in the HF and stage 2 in the LF for *E. globulus* branches. However, this distribution was not as clearly observed for the fractions obtained from *E. globulus* leaves, indicating a distinct behavior in the distribution of these compounds depending on the biomass type used.

Although the findings provide valuable insights into the effects of fractionated condensation on bio-oil chemical composition, further investigations are warranted. Future studies should explore derivatization techniques for improved compound identification, as well as semi-quantitative and quantitative analyses of the major chemical compounds. Such research could deepen the understanding of fractionation mechanisms and support the identification of more specific and suitable applications for each fraction, as suggested by Vilas Boas *et al.* [47].

3.7. Heavy bio-oil vs. typical liquid fossil fuels and biofuels

A comparative analysis of the O/C and H/C molar ratios (Fig. 12) and the heating value (Fig. 13) of HFs of bio-oil collected in the two condensation systems studied, FCS and SCS, is presented. These properties are compared with those of commonly used liquid fuels, including fossil fuels and biofuels.

The O/C molar ratios of HF from the FCS were significantly lower than those of HF from SCS, indicating that FCS improved bio-oil quality by separating fractions with lower oxygen concentration. However, despite this improvement, the O/C molar ratios of these HFs remain considerably higher than those of fossil fuels. This can be attributed to the presence of water in several condensation stages (particularly in stages 2,3 and 4) and the high concentration of oxygenated compounds.

Among the analyzed bio-oil fractions, the HF collected in stage 1 of the FCS during the pyrolysis of *E. globulus* leaves and branches exhibited an O/C ratio closer to that of biodiesel, and trending towards values observed for fossil fuels. The HF derived from *E. globulus* leaves showed the highest similarity. Despite this, the oxygen concentration of these fractions remains a limiting factor for direct use as fuel, as elevated oxygen levels reduce combustion efficiency and compromise fuel stability.

One of the advantages of FCS lies in its ability to generate fractions that may require fewer upgrading steps compared to those obtained via conventional single-stage condensation systems. This characteristic could facilitate the application of downstream upgrading techniques, such as hydroprocessing, in a more targeted and energy-efficient manner. Alternatively, co-feeding bio-oil HF into existing petroleum refining units, such as Fluid Catalytic Cracking, could be explored.

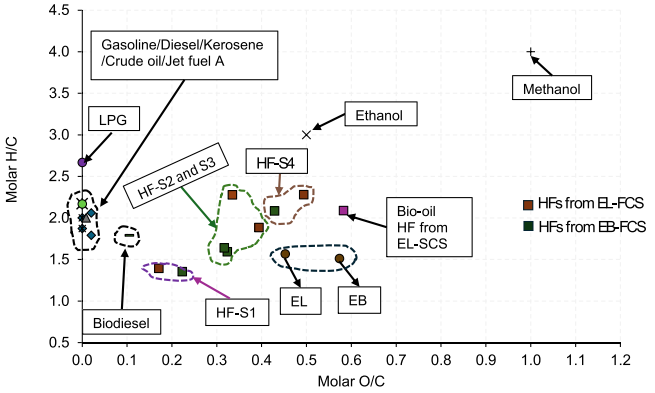

Fig. 12. Van Krevelen diagram for the heavy fractions of raw bio-oil collected in fractional condensation system (stage 1–4) and the single-stage condensation system, from *E. globulus* leaves and branches pyrolysis, original biomass, and typical liquid fuels.

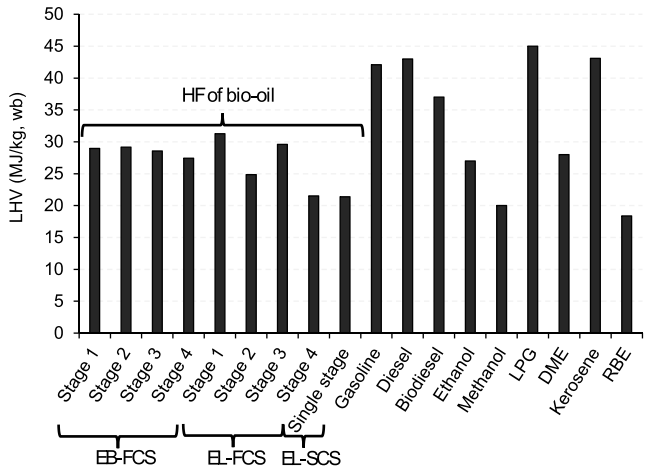

Fig. 13. Lower heating value of heavy fractions of raw bio-oil collected in fractional condensation system (stage 1–4) and the single-stage condensation system, from *E. globulus* leaves and branches pyrolysis, original biomass (RBE), and typical liquid fuels.

However, this approach requires further investigation, as the addition of HF may lead to coke formation on the catalyst, potentially reducing process yields depending on bio-oil and fossil fuels interactions.

Regarding the heating value, the HFs of bio-oil have a LHV (wb) than methanol and the original biomass (RBE) and are comparable to or even exceed dimethyl ether (DME) and ethanol, depending on the condensation stage (Fig. 13). However, these LHV values remain significantly lower than those of conventional fuels.

4. Conclusions

This study evaluated the fractional condensation system of pyrolysis vapors from residual *E. globulus* biomass using a prototype-scale auger reactor, comparing its performance with a conventional single-stage condensation system. The FCS consisted of four condensation stages arranged in series and operating at different temperatures, designed to separate bio-oil fractions with higher quality, lower water and oxygen concentration, higher heating value, and distinct physicochemical properties.

Results showed that FCS maintained condensation efficiency and pyrolysis product yields comparable to SCS, but offered significant advantages in its ability to recover heavy bio-oil fractions with lower water concentration. In particular, the HF collected in stage 1 of the FCS had low water concentration between 3 % and 6 %wt., reduced oxygen concentration between 17 % and 21 %wt., higher carbon concentration between 69 % and 72 %wt and O/C molar ratio close to that of biodiesel, although they represented only a small portion of the total bio-oil yield. These fractions also exhibited high heating values, reaching up to 31 MJ/kg of bio-oil (wb). These findings highlight the potential of these bio-oil fractions as liquid fuels for direct use in industrial boilers or as intermediate feedstock for the synthesis of advanced biofuels, requiring fewer processing steps or resources compared to the HFs produced by the SCS.

Additionally, a spontaneous fraction separation between HF and LF was observed immediately after collection in both the FCS (except stage 1) and the SCS, a phenomenon rarely addressed in literature. This immediate separation, possibly influenced by operational conditions (biomass type, pyrolysis temperature, operating conditions of the condensations system), may facilitate efficient and simplified aqueous fraction removal from the organic fraction.

The LF, especially those collected in stages 3 and 4 of the FCS, exhibited high water concentration (>80 %wt.), limiting their direct applicability as fuels. However, these fractions show potential for alternative uses, such as substrates for anaerobic digestion, formulation of pesticides, and extraction of high-value compounds (e.g., levoglucosan, acetic acid).

Despite its promising performance, the FCS did not enable fully selective chemical separation of functional groups across the condensation stages, likely due to the formation of azeotropic mixtures and intermolecular interactions during vapor condensation. Nevertheless, certain trends were observed: an increased relative content of acids in the intermediate LF stages (2 and 3), retention of phenolic compounds in the early stages, in both HF and LF, particularly from *E. globulus* branches and the accumulation of furanic compounds in the final stage.

Future studies should focus on optimizing FCS operating parameters (e.g., temperature gradients and number of stages), to enhance yield and stability of desirable bio-oil fractions. Moreover, the long-term stability and aging behavior of the separated fractions should be assessed under realistic storage conditions. Detailed chemical characterization, including the absolute quantification of bio-oil compounds, is essential to fully understand the molecular composition and functional group distribution of each fraction, and to evaluate their suitability for energy and industrial applications. Further investigation into the integration of fractional condensation with modular pyrolysis systems, along with techno-economic assessments, would also support its scale-up as a cleaner and more efficient biomass valorization strategy.

CRediT authorship contribution statement

A.C.M. Vilas-Boas: Conceptualization, Formal analysis, Investigation, Methodology, Visualization, Writing – original draft, Writing – review and editing. **L.A.C. Tarelho:** Conceptualization, Resources, Supervision, Writing – review and editing, Funding acquisition. **C.C. Marques:** Investigation, Methodology. **J.M.O Moura:** Investigation, Writing – review and editing. **M.C. Santos:** Investigation. **F. Paradela:** Investigation. **M.I. Nunes:** Supervision, Writing – review and editing. **A. J.D. Silvestre:** Supervision, Writing – review and editing.

Declaration of Competing Interest

The authors declare that they have no known competing financial interests or personal relationships that could have appeared to influence the work reported in this paper.

Acknowledgments

It is acknowledged the financial support from Project BioValChar - Sustainable valorization of residual biomass for biochar, PCIF-GVB-0034-2019, http://doi.org/10.54499/PCIF/GVB/0034/2019, funded by the Portuguese Foundation for Science and Technology (FCT), and Project Inpactus – innovative products and technologies from eucalyptus, Project N.º 21874, POCI-01–0247-FEDER-021874, funded by Portugal 2020 through European Regional Development Fund (ERDF) in the frame of COMPETE 2020 nº246/AXIS II/2017. This work is funded by national funds through FCT – Fundação para a Ciência e a Tecnologia I.P., to CESAM – Centre for Environmental and Marine Studies under the project/grant UID/50006 + LA/P/0094/2020 (doi.org/10.54499/LA/P/0094/2020), and CICECO-Aveiro Institute of Materials, UIDB/50011/2020 (DOI 10.54499/UIDB/50011/2020) & LA/P/0006/2020 (DOI 10.54499/LA/P/0006/2020).

The authors also acknowledge the FCT for providing financial support to the PhD scholarships granted to Ana C. M. Vilas Boas (ref. 2021.08162.BD) and Catarina C. Marques (ref. 2021.08959.BD).

Appendix A. Supporting information

Supplementary data associated with this article can be found in the online version at doi:10.1016/j.jaap.2025.107329.

Data Availability

All relevant data supporting this study are included in this paper and its supplementary material.

References

[1] European Commission. EFFIS Estimates for European Union: Fires mapped in EFFIS of approx. 30 ha or larger n.d. ⟨https://forest-fire.emergency.copernicus.eu/apps/effis.statistics/estimates⟩ (accessed May 2, 2025).

[2] Instituto da Conservação da Natureza e das Florestas (ICNF). 8.° Relatório provisório de incêndios rurais – 2024. 2024.

[3] ECO. Fogos custaram 377,2 milhões de euros a Portugal em 2023, avalia o Banco Mundial 2024. ⟨https://eco.sapo.pt/2024/05/15/fogos-custaram-3772-milhoes-de-euros-a-portugal-em-2023-avalia-o-banco-mundial/?utm_source=chatgpt.com⟩ (accessed May 2, 2025).

[4] BBC. Portugal's wildfire that broke a community 2018. ⟨https://www.bbc.com/news/world-europe-44438505⟩ (accessed May 1, 2025).

[5] Agência Portuguesa do Ambiente (APA). Memorando sobre emissões GEE: Inventário Nacional de Emissões 2024. 2024.

[6] Instituto da Conservação da Natureza e das Florestas (ICNF). Perfil Florestal - Portugal. 2021.

[7] Medidas de Eficiência Energética em Sistemas Industriais (MEESI). Pasta e Papel n. d. ⟨https://www.meesi.pt/medidas-setor/pasta-e-papel⟩ (accessed May 1, 2025).

[8] G. Pena-Vergara, L.R. Castro, C.A. Gasparetto, W.A. Bizzo, Energy from planted forest and its residues characterization in Brazil, Energy 239 (2022) 122243, https://doi.org/10.1016/j.energy.2021.122243.

[9] A. Bhatt, V. Ravi, Y. Zhang, G. Heath, R. Davis, E.C.D. Tan, Emission factors of industrial boilers burning biomass-derived fuels, J. Air Waste Manag. Assoc. 73 (2023) 241–257, https://doi.org/10.1080/10962247.2023.2166158.

[10] D.T. Pio, A.C.M. Vilas-Boas, N.F.C. Rodrigues, A. Mendes, Carbon neutral methanol from pulp mills towards full energy decarbonization: an inside perspective and critical review, Green. Chem. 24 (2022) 5403–5428, https://doi.org/10.1039/d2gc01528e.

[11] D.T. Pio, L.A.C. Tarelho, P.C.R. Pinto, Gasification-based biorefinery integration in the pulp and paper industry: a critical review, Renew. Sustain. Energy Rev. 133 (2020) 110210, https://doi.org/10.1016/j.rser.2020.110210.

[12] Nations United Development Programme. The 17 goals | Sustainable Development n.d. ⟨https://www.undp.org/sustainable-development-goals?gclid=CjwKCAjw3oqoBhAjEiwA_UaLtp3SU5xvGk0HNPhFx8D-2cm0em2MjOGD2LLHaAH80aTAhkP5bDEyfRoCmZAQAvD_BwE⟩ (accessed September 14, 2023).

[13] Commission E. REPowerEU: affordable, secure and sustainable energy for Europe n.d. ⟨https://commission.europa.eu/strategy-and-policy/priorities-2019-2024/european-green-deal/repowereu-affordable-secure-and-sustainable-energy-europe_en⟩ (accessed July 14, 2024).

[14] European Parliament, Council of the Union European. EU climate law. Sustainable Finance and Climate Change: Law and Regulation 2021.

[15] D. Lachos-Perez, J.C. Martins-Vieira, J. Missau, K. Anshu, O.K. Siakpebru, S. K. Thengane, et al., Review on biomass pyrolysis with a focus on Bio-Oil upgrading techniques, Analytica 4 (2023) 182–205, https://doi.org/10.3390/analytica4020015.

[16] Basu P. Biomass gasification and pyrolysis: Practical design. 2010.

[17] S. Czernik, A.V. Bridgwater, Overview of applications of biomass fast pyrolysis oil, Energy Fuels 18 (2004) 590–598, https://doi.org/10.1021/ef034067u.

[18] M. Guo, W. Song, J. Buhain, Bioenergy and biofuels: history, status, and perspective, Renew. Sustain. Energy Rev. 42 (2015) 712–725, https://doi.org/10.1016/j.rser.2014.10.013.

[19] IRENA, Reaching zero with renewables - biojet fuels, The International Renewable Energy Agency, 2021.

[20] IRENA. Innovation Technology Outlook for Advanced Liquid Biofuels. International Renewable Energy Agency 2016.

[21] Y. Zhang, S. Fan, T. Liu, M.M. Omar, B. Li, Perspectives into intensification for aviation oil production from microwave pyrolysis of organic wastes, Chem. Eng. Process. Process. Intensif. 176 (2022) 108939, https://doi.org/10.1016/j.cep.2022.108939.

[22] B.J. Álvarez-Chávez, S. Godbout, V. Raghavan, Effect of fractional condensation system coupled with an auger pyrolizer on bio-oil composition and properties, J. Anal. Appl. Pyrolysis 158 (2021), https://doi.org/10.1016/j.jaap.2021.105270.

[23] C.S. Fermanelli, A. Córdoba, L.B. Pierella, C. Saux, Pyrolysis and copyrolysis of three lignocellulosic biomass residues from the agro-food industry: a comparative study, Waste Manag. 102 (2020) 362–370, https://doi.org/10.1016/j.wasman.2019.10.057.

[24] S. Stelmach, K. Ignasiak, A. Czardybon, J. Bigda, Evaluation of Bio-Oils in terms of fuel properties, Processes 11 (2023), https://doi.org/10.3390/pr11123317.

[25] Y.H. Chan, S.K. Loh, B.L.F. Chin, C.L. Yiin, B.S. How, K.W. Cheah, et al., Fractionation and extraction of bio-oil for production of greener fuel and value-added chemicals: recent advances and future prospects, Chem. Eng. J. 397 (2020) 125406, https://doi.org/10.1016/j.cej.2020.125406.

[26] S. Ren, X.P. Ye, A.P. Borole, Separation of chemical groups from bio-oil water-extract via sequential organic solvent extraction, J. Anal. Appl. Pyrolysis 123 (2017) 30–39, https://doi.org/10.1016/j.jaap.2017.01.004.

[27] C. Wang, Z. Luo, R. Diao, X. Zhu, Study on the effect of condensing temperature of walnut shells pyrolysis vapors on the composition and properties of bio-oil, Bioresour. Technol. 285 (2019) 121370, https://doi.org/10.1016/j.biortech.2019.121370.

[28] A. Mati, M. Buffi, S. Dell'orco, G. Lombardi, P.M. Ruiz Ramiro, S.R.A. Kersten, et al., Fractional condensation of fast pyrolysis Bio-Oil to improve biocrude quality towards alternative fuels production, Appl. Sci. (Switz.) 12 (2022), https://doi.org/10.3390/app12104822.

[29] A.C. Johansson, K. Iisa, L. Sandström, H. Ben, H. Pilath, S. Deutch, et al., Fractional condensation of pyrolysis vapors produced from nordic feedstocks in cyclone pyrolysis, J. Anal. Appl. Pyrolysis 123 (2017) 244–254, https://doi.org/10.1016/j.jaap.2016.11.020.

[30] R.J.M. Westerhof, D.W.F. Brilman, M. Garcia-Perez, Z. Wang, S.R.G. Oudenhoven, W.P.M. Van Swaaij, et al., Fractional condensation of biomass pyrolysis vapors, Energy Fuels 25 (2011) 1817–1829, https://doi.org/10.1021/ef2000322.

[31] A. Tumbalam Gooty, D. Li, C. Briens, F. Berruti, Fractional condensation of bio-oil vapors produced from birch bark pyrolysis, Sep. Purif. Technol. 124 (2014) 81–88, https://doi.org/10.1016/j.seppur.2014.01.003.

[32] M. Siriwardhana, Fractional condensation of pyrolysis vapours as a promising approach to control bio-oil aging: dry birch bark bio-oil, Renew. Energy 152 (2020) 1121–1128, https://doi.org/10.1016/j.renene.2020.01.095.

[33] M. Siriwardhana, Fractional condensation of pyrolysis vapours as a promising approach to control bio-oil aging: dry birch bark bio-oil, Renew. Energy 152 (2020) 1121–1128, https://doi.org/10.1016/j.renene.2020.01.095.

[34] J. Xu, N. Brodu, L. Abdelouahed, B. Taouk, Investigation of the combination of fractional condensation and water extraction for improving the storage stability of pyrolysis bio-oil, Fuel 314 (2022), https://doi.org/10.1016/j.fuel.2021.123019.

[35] S. Chai, B.S. Kang, B. Valizadeh, S. Valizadeh, J. Hong, J. Jae, et al., Fractional condensation of bio-oil vapors from pyrolysis of various sawdust wastes in a bench-scale bubbling fluidized bed reactor, Chemosphere 350 (2024) 141121, https://doi.org/10.1016/j.chemosphere.2024.141121.

[36] B.J. Álvarez-Chávez, S. Godbout, É. Le Roux, J.H. Palacios, V. Raghavan, Bio-oil yield and quality enhancement through fast pyrolysis and fractional condensation concepts, Biofuel Res. J. 6 (2019) 1054–1064, https://doi.org/10.18331/BRJ2019.6.4.2.

[37] S.S. Liaw, V.H. Perez, R.J.M. Westerhof, G.F. David, C. Frear, M. Garcia-Perez, Biomethane production from pyrolytic aqueous phase: biomass acid washing and condensation temperature effect on the Bio-oil and aqueous phase composition, Bioenergy Res. 13 (2020) 878–886, https://doi.org/10.1007/s12155-020-10100-3.

[38] N. Li, W. Yi, Z. Li, L. Wang, Y. Li, X. Bai, et al., Pyrolysis of rice husk in a fluidized bed reactor: evaluate the characteristics of fractional bio-oil and particulate emission of carbonaceous aerosol (CA), J. Renew. Mater. 8 (2020) 329–346, https://doi.org/10.32604/jrm.2020.08618.

[39] É. Le Roux, S. Barnabé, S. Godbout, I. Zamboni, J. Palacios, Production and characterization of two fractions of pyrolysis liquid from agricultural and wood residues, Biomass.. Convers. Biorefinery 12 (2022) 3333–3343, https://doi.org/10.1007/s13399-020-01015-2.

[40] S. Valizadeh, D. Oh, J. Jae, S. Pyo, H. Jang, H. Yim, et al., Effect of torrefaction and fractional condensation on the quality of bio-oil from biomass pyrolysis for fuel applications, Fuel 312 (2022) 122959, https://doi.org/10.1016/j.fuel.2021.122959.

[41] B.J. Álvarez-Chávez, S. Godbout, V. Raghavan, Effect of fractional condensation system coupled with an auger pyrolizer on bio-oil composition and properties, J. Anal. Appl. Pyrolysis 158 (2021), https://doi.org/10.1016/j.jaap.2021.105270.

[42] S. Papari, K. Hawboldt, P. Fransham, Study of selective condensation for woody biomass pyrolysis oil vapours, Fuel 245 (2019) 233–239, https://doi.org/10.1016/j.fuel.2019.02.055.

[43] S.A. Channiwala, P.P. Parikh, A unified correlation for estimating HHV of solid, liquid and gaseous fuels, Fuel 81 (2002) 1051–1063, https://doi.org/10.1016/S0016-2361(01)00131-4.

[44] M. Santos, A.C. Morim, M. Videira, F. Silva, M. Matos, L.A.C. Tarelho, Characteristics of biochar obtained by pyrolysis of residual forest biomass at different process scales, Energies 17 (2024), https://doi.org/10.3390/en17194861.

[45] A.C.M. Vilas-Boas, L.A.C. Tarelho, H.S.M. Oliveira, F.G.C.S. Silva, D.T. Pio, M.A. A. Matos, Valorisation of residual biomass by pyrolysis: influence of process conditions on products, Sustain. Energy Fuels 8 (2023) 379–396, https://doi.org/10.1039/d3se01216f.

[46] J. Xu, N. Brodu, J. Wang, L. Abdelouahed, B. Taouk, Chemical characteristics of bio-oil from beech wood pyrolysis separated by fractional condensation and water extraction, J. Energy Inst. 99 (2021) 186–197, https://doi.org/10.1016/j.joei.2021.09.006.

[47] A.C.M. Vilas-Boas, L.A.C. Tarelho, J.M.O. Moura, H.G.M.F. Gomes, C.C. Marques, D.T. Pio, et al., Methodologies for bio-oil characterization from biomass pyrolysis: a review focused on GC-MS, J. Anal. Appl. Pyrolysis 185 (2025) 106850, https://doi.org/10.1016/j.jaap.2024.106850.

[48] W. Yi, X. Wang, K. Zeng, H. Yang, J. Shao, S. Zhang, et al., Improving bio-oil stability by fractional condensation and solvent addition, Fuel 290 (2021) 119929, https://doi.org/10.1016/j.fuel.2020.119929.

[49] C. Wang, Z. Luo, S. Li, X. Zhu, Coupling effect of condensing temperature and residence time on bio-oil component enrichment during the condensation of biomass pyrolysis vapors, Fuel 274 (2020) 117861, https://doi.org/10.1016/j.fuel.2020.117861.

[50] Y. Han, M. Gholizadeh, C.C. Tran, S. Kaliaguine, C.Z. Li, M. Olarte, et al., Hydrotreatment of pyrolysis bio-oil: a review, Fuel Process. Technol. 195 (2019), https://doi.org/10.1016/j.fuproc.2019.106140.

[51] C. Wang, Y. Yang, Y. Ma, X. Zhu, Experimental study on the composition evolution and selective separation of biomass pyrolysis vapors in the four-staged indirect heat exchangers, Bioresour. Technol. 332 (2021) 125115, https://doi.org/10.1016/j.biortech.2021.125115.
[52] L. Fagernas, Chemical and physical characterization of Biomass-Based pyrolysis oils, VTT Energy (1995) 120.
[53] Q. Lu, W.Z. Li, X.F. Zhu, Overview of fuel properties of biomass fast pyrolysis oils, Energy Convers. Manag. 50 (2009) 1376–1383, https://doi.org/10.1016/j.enconman.2009.01.001.
[54] A.J.D. Silvestre, J.A.S. Cavaleiro, B. Delmond, C. Filliatre, G. Bourgeois, Analysis of the variation of the essential oil composition of eucalyptus globulus labill. From Portugal using multivariate statistical analysis, Ind. Crops Prod. 6 (1997) 27–33, https://doi.org/10.1016/S0926-6690(96)00200-2.
[55] E. Lazzari, K. Arena, E.B. Caramão, M. Herrero, Quantitative analysis of aqueous phases of bio-oils resulting from pyrolysis of different biomasses by two-dimensional comprehensive liquid chromatography, J. Chromatogr. A 1602 (2019) 359–367, https://doi.org/10.1016/j.chroma.2019.06.016.
[56] M. Matos, B.D. Mattos, P.H.G. de Cademartori, T.V. Lourençon, F.A. Hansel, P.R. S. Zanoni, et al., Pilot-Scaled Fast-Pyrolysis conversion of eucalyptus wood fines into products: discussion toward possible applications in biofuels, materials, and precursors, Bioenergy Res. 13 (2020) 411–422, https://doi.org/10.1007/s12155-020-10094-y.
[57] J. Xu, S. Zhang, Y. Shi, P. Zhang, D. Huang, C. Lin, et al., Upgrading the wood vinegar prepared from the pyrolysis of biomass wastes by hydrothermal pretreatment, Energy 244 (2022) 122631, https://doi.org/10.1016/j.energy.2021.122631.
[58] X. Liu, J. Wang, X. Feng, J. Yu, Wood vinegar resulting from the pyrolysis of apple tree branches for annual bluegrass control, Ind. Crops Prod. 174 (2021) 114193, https://doi.org/10.1016/j.indcrop.2021.114193.
[59] A.P. Pinheiro Pires, J. Arauzo, I. Fonts, M.E. Domine, A. Fernández Arroyo, M. E. Garcia-Perez, et al., Challenges and opportunities for bio-oil refining: a review, Energy Fuels 33 (2019) 4683–4720, https://doi.org/10.1021/acs.energyfuels.9b00039.
[60] I. Junior, M. Do Nascimento, R. De Souza, A. Dufour, R. Wojcieszak, Levoglucosan: a promising platform molecule? Green. Chem. 22 (2020) 5859–5880, https://doi.org/10.1039/d0gc01490g.
[61] T. Sarchami, N. Batta, F. Berruti, Production and separation of acetic acid from pyrolysis oil of lignocellulosic biomass: a review, Biofuels Bioprod. Bioref. 15 (2021) 1912–1937, https://doi.org/10.1002/bbb.2273.
[62] A.P. Pinheiro Pires, J. Arauzo, I. Fonts, M.E. Domine, A. Fernández Arroyo, M. E. Garcia-Perez, et al., Challenges and opportunities for bio-oil refining: a review 33 (2019), https://doi.org/10.1021/acs.energyfuels.9b00039.
[63] V. Paasikallio, J. Kihlman, C.A.S. Sánchez, P. Simell, Y. Solantausta, J. Lehtonen, Steam reforming of pyrolysis oil aqueous fraction obtained by one-step fractional condensation, Int. J. Hydrog. Energy 40 (2015) 3149–3157, https://doi.org/10.1016/j.ijhydene.2015.01.025.
[64] J. Justicia, J.A. Baeza, L. Calvo, F. Heras, M.A. Gilarranz, Valorization to hydrogen of bio-oil aqueous fractions from lignocellulosic biomass pyrolysis by aqueous phase reforming over Pt/C catalyst, Chem. Eng. J. 477 (2023), https://doi.org/10.1016/j.cej.2023.146860.